



Development and validation of a low-cost polymer selective laser sintering machine



Martin Mapley^{a,b,*}, Yidi Lu^{b,c}, Shaun D. Gregory^{a,b,d}, Jo P. Pauls^{a,b}, Geoff Tansley^{a,b}, Andrew Busch^a

^a School of Engineering and Built Environment, Griffith University, Queensland, Australia

^b Innovative Cardiovascular Engineering and Technology Laboratory, The Prince Charles Hospital, Brisbane, Queensland, Australia

^c University of Queensland, Brisbane, Queensland, Australia

^d Department of Mechanical and Aerospace Engineering, Monash University, Melbourne, Victoria, Australia

ARTICLE INFO

Article history:

Received 23 April 2020

Received in revised form 22 June 2020

Accepted 22 June 2020

Keywords:

Additive manufacturing

3D printing

Powder bed fusion

Thermal control

Laser diode

Polymer

ABSTRACT

Due to manufacturer implemented processing parameter restrictions and the cost prohibitive nature of selective laser sintering (SLS) machines, researchers have limited opportunities to explore the processing of new materials using this additive manufacturing (3D printing) process. Accordingly, this article aimed to overcome these limitations by describing the build and operation of a customizable low-cost polymer SLS machine. The machine boasts a three piston powder bed with the center build piston heated by PID controlled ceramic heaters. Thermal energy for powder consolidation was provided via a 2.44 W solid state diode laser which was mechanically traversed using stepper motor driven belt drives. New layers of powder were deposited by a counter-rotating roller system. The SLS machine was controlled by executing G-code in Mach3 allowing full customization of processing parameters. The machine demonstrated the production of parts from polyamide-12 reaching densities of $918 \pm 9 \text{ kg/m}^3$ while achieving an elastic modulus of $358.36 \pm 3.04 \text{ MPa}$ and elongation at break of $11.13 \pm 0.02\%$. With part properties similar to those achievable with a commercial machine, this low-cost SLS machine could be a vital tool in assisting researchers to explore the processing of new materials.

© 2020 The Author(s). Published by Elsevier Ltd. This is an open access article under the CC BY-NC-ND license (<http://creativecommons.org/licenses/by-nc-nd/4.0/>).

Specifications table:

| | |
|------------------------|---|
| Hardware name | Selective Laser Sintering Machine |
| Subject area | <ul style="list-style-type: none"> • Engineering and Material Science |
| Hardware type | <ul style="list-style-type: none"> • Electrical engineering and computer science • Mechanical engineering and materials science |
| Open Source License | CC BY 4.0 |
| Cost of Hardware | \$1,162.32 - AUD |
| Source File Repository | https://doi.org/10.17605/OSF.IO/YKSPG |

* Corresponding author.

E-mail address: mmapley@gmail.com (M. Mapley).

<https://doi.org/10.1016/j.ohx.2020.e00119>

2468-0672/© 2020 The Author(s). Published by Elsevier Ltd.

This is an open access article under the CC BY-NC-ND license (<http://creativecommons.org/licenses/by-nc-nd/4.0/>).

1. Hardware in context

Additive manufacturing (AM), colloquially known as 3D printing, is a technique where parts are formed from materials in a layer-by-layer fashion based on information provided by a computer aided design (CAD) file. Recently there has been growing interest in AM processes as parts can be rapidly prototyped which leads to significant reductions in product development costs and time to market [1]. Of specific interest is a powder-based AM manufacturing process known as selective laser sintering (SLS). The SLS process involves directing the beam of a high-powered laser over a thin layer of powder which is selectively consolidated by traversing the beam in the required pattern. On the completion of consolidation of the powder layer, further layers are subsequently added and the consolidation repeated until a 3D part is produced which resembles the CAD file. A diagram showing the essential components of an SLS machine is shown in Fig. 1.

While many materials (ceramics, metals and polymers) can be processed using SLS, a vast majority of machines use pure or alloys of polyamide-12 as the feedstock [2]. The growing popularity of polymer SLS is due to several inherent advantages of the process such as the absence of the requirement for support material, the high densities achievable and the isotropic mechanical properties of the parts [3]. However, despite there being a multitude of commercial SLS systems available, their high cost and low flexibility to process non-manufacturer specified materials limits their widespread use for the experimental processing of new and existing materials. Although recently there has been increasing interest in reducing the cost of SLS systems with some companies releasing systems capable of processing polymers for less than AUD\$10,000, they still do not allow flexibility in low level control of processing parameters [4]. Therefore, this article provides the necessary information for researchers to construct and operate a customisable SLS machine which is capable of producing high quality parts from polymer-based materials.

2. Hardware description

This low-cost SLS machine was designed to give users complete control over all of the processing parameters which contribute to material consolidation enabling different processing strategies to be implemented depending on the material being processed. The following section briefly describes the function of each major component within the SLS machine.

2.1. Radiation source and positioning system

To supply the required optical energy to selectively sinter particles on the surface of the powder bed, a 15 W (manufacturer rated peak power) laser diode (LMC450B, EleksMaker, Hong Kong, China) was chosen that emits light radiation at a wavelength of 450 nm. Laser diodes are inherently more robust and compact than other forms of laser modules (such as CO₂) which alleviates the need for complex and expensive scanning systems, such as galvanically controlled mirrors, as the laser can be tracked directly over the powder bed. Therefore to traverse the laser diode, a belt-driven overhead gantry design was adopted (Fig. 2).

2.2. Powder bed

A powder bed in its simplest form is comprised of one or more pistons, one of which serves as the build platform with the others serving as powder feeders and/or to collect excess material. A simple design involving three adjacent pistons was chosen (Fig. 3). The outside pistons were designated as powder feeders which contain the virgin material to be deposited on the

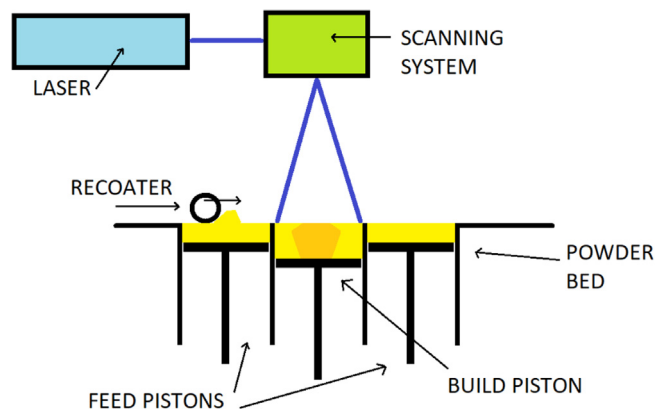


Fig. 1. Primary components of a selective laser sintering machine.

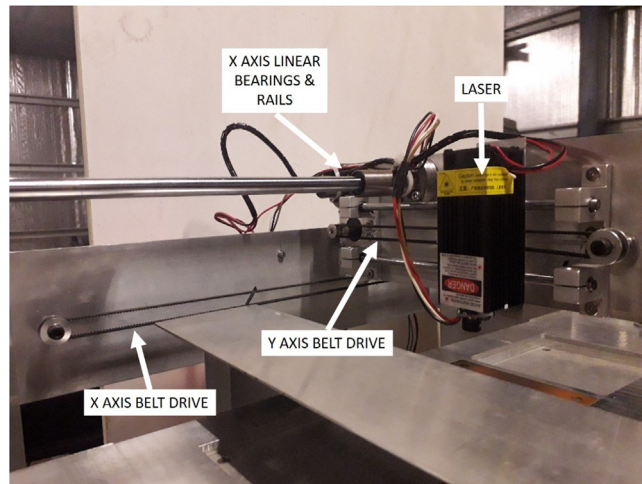


Fig. 2. Laser and positioning system.

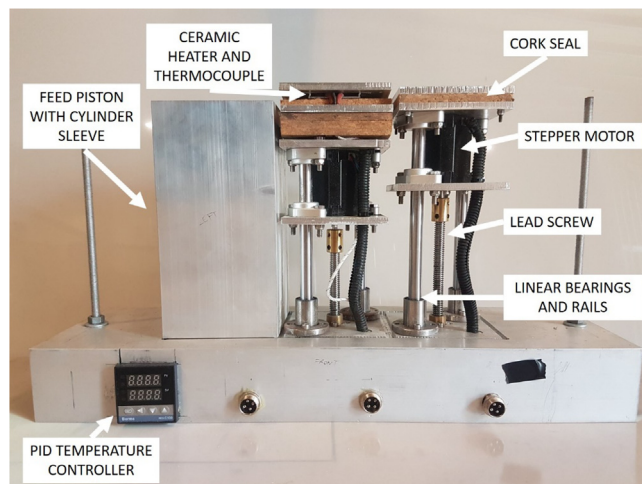


Fig. 3. Powder bed with build platform (center) and right feed piston sleeve removed.

build platform by the recoater. The center piston was designed as the build platform in which virgin material was deposited and then selectively consolidated by the laser.

2.3. Recoater

In order to apply another layer of powder to the build platform after the fusion of each layer, a counter-rotating roller was attached to linear rails suspended above the pistons (Fig. 4).

2.4. Hardware

A hardware interface (Fig. 5) was required to convert the low voltage signals from the computer into drive currents for the motors. The stepper and DC motor drivers were optically isolated from the computer's parallel ports via interface cards to avoid damage to components of the computer.

2.5. Control software

The system was controlled using a hobbyist CNC control application known as Mach3 (Newfangled Solutions LLC, Livermore Falls, Maine, USA) (Fig. 6). This allowed real-time adjustment of processing parameters via the graphical user interface as well as pre-processing adjustment of parameters by editing the input instruction set (G-code). Although not open-source

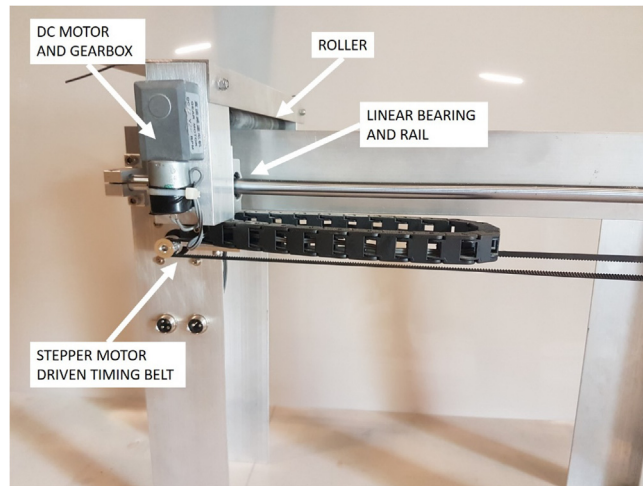


Fig. 4. Recoater setup for deposition of new powder layers on the build piston.

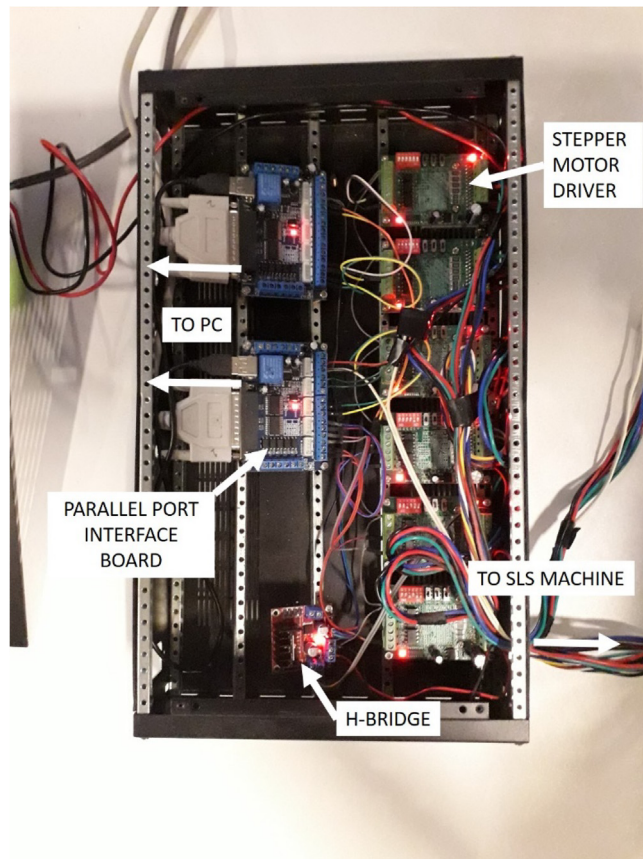


Fig. 5. Parallel port interface system.

software, the freely available trial version allows full program usage with execution of up to 500 lines of G-code which is enough for some small models. The G-code instructions were generated from model data using Slic3er (Alessandro Ranelucci, Rome, Italy) and then modified for compatibility with the SLS process by a MATLAB (Mathworks, Natick, Massachusetts, USA) or Scilab (Scilab Enterprises, Orsay, France) script.

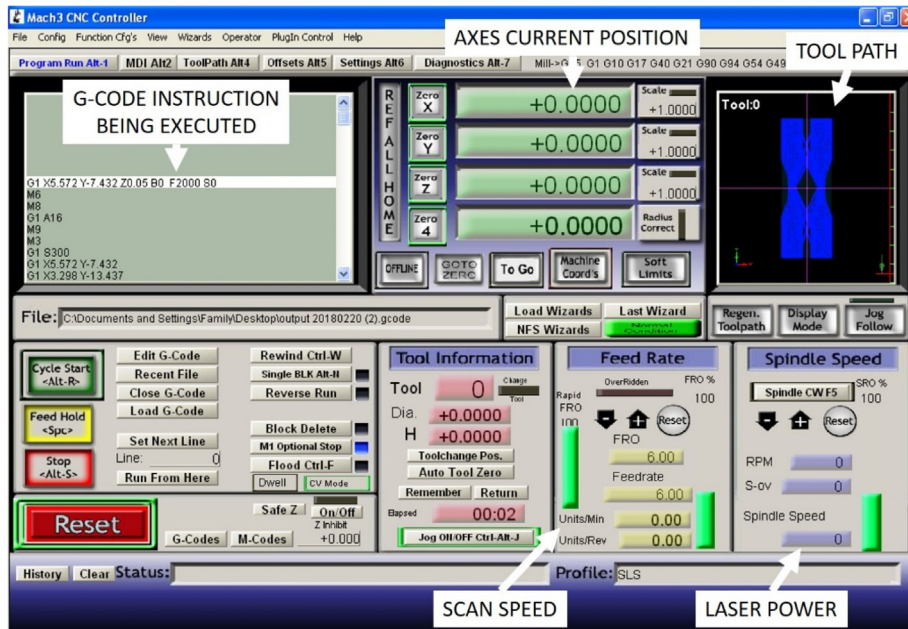


Fig. 6. Mach3 graphical user interface.

3. Design files

3.1. Design files summary

| Design file name | File type | Open source license | Location of the file |
|---------------------------------------|---------------|---------------------|---|
| final_assembly.sldasm | CAD | CC BY 4.0 | https://doi.org/10.17605/OSF.IO/YKSPG |
| pid_temp.jpg | Image | CC BY 4.0 | https://doi.org/10.17605/OSF.IO/YKSPG |
| system.jpg | Image | CC BY 4.0 | https://doi.org/10.17605/OSF.IO/YKSPG |
| gcode_conversion_script_flowchart.jpg | Image | CC BY 4.0 | https://doi.org/10.17605/OSF.IO/YKSPG |
| gcode_sls_transform2.m | MATLAB script | CC BY 4.0 | https://doi.org/10.17605/OSF.IO/YKSPG |
| C_gantry_part_i.dxf | CAD | CC BY 4.0 | https://doi.org/10.17605/OSF.IO/YKSPG |
| D_gantry_part_i.dxf | CAD | CC BY 4.0 | https://doi.org/10.17605/OSF.IO/YKSPG |
| E_gantry_part_ii.dxf | CAD | CC BY 4.0 | https://doi.org/10.17605/OSF.IO/YKSPG |
| F_gantry_part_ii.dxf | CAD | CC BY 4.0 | https://doi.org/10.17605/OSF.IO/YKSPG |
| H_powder_bed.dxf | CAD | CC BY 4.0 | https://doi.org/10.17605/OSF.IO/YKSPG |
| I_powder_bed.dxf | CAD | CC BY 4.0 | https://doi.org/10.17605/OSF.IO/YKSPG |
| J_powder_bed.dxf | CAD | CC BY 4.0 | https://doi.org/10.17605/OSF.IO/YKSPG |
| K_powder_bed.dxf | CAD | CC BY 4.0 | https://doi.org/10.17605/OSF.IO/YKSPG |

(continued on next page)

(continued)

| Design file name | File type | Open source license | Location of the file |
|------------------|-----------|---------------------|---|
| L_powder_bed.dxf | CAD | CC BY 4.0 | YKSPG https://doi.org/10.17605/OSF.IO/YKSPG |
| N_powder_bed.dxf | CAD | CC BY 4.0 | https://doi.org/10.17605/OSF.IO/YKSPG |
| O_powder_bed.dxf | CAD | CC BY 4.0 | https://doi.org/10.17605/OSF.IO/YKSPG |

- Final assembly – CAD file showing the assembled machine. This file is supplementary to the photographs and mill profiles so that the machine can be viewed from perspectives not shown in the document.
- PID temperature controller circuit diagram – shows the connections required for the PID temperature controller and the ceramic heaters.
- System circuit diagram – shows the connections for the hardware interface system between the computer and the motors/laser.
- G-code conversion flowchart – designed to accompany the MATLAB script for G-code conversion.
- G-code SLS transform – MATLAB script which converts the G-code which is output from Slic3r from fused deposition modelling into SLS.
- All of the .dxf CAD files are mill profiles for the corresponding aluminium parts that make up the frame of the machine.

4. Bill of materials

4.1. Bill of materials

The extruded aluminium sections are of standard dimensions and should be available from most aluminium suppliers. All of the fixing hardware (bolts and nuts) is available at any hardware store.

| Designator | Component | Number | Cost per unit - currency | Total cost - currency | Source of materials | Material type |
|---|--|--------|--------------------------|-----------------------|-----------------------|---------------|
| Electrical Components | | | | | | |
| Computer | Windows XP/ Vista PC | 1 | | | Recycled | Other |
| Gantry Part II | LMC450B Laser Module | 1 | \$167 - AUD | \$167 - AUD | eBay.com.au | Other |
| Computer | DB25 Parallel Port PCI Controller (CH351Q) | 1 | \$5.83 - AUD | \$5.83 - AUD | eBay.com.au | Other |
| Control Box | 24 VDC Power Supply (5A) | 1 | \$17.99 - AUD | \$17.99 - AUD | eBay.com.au | Other |
| Control Box | LPT Port Breakout Board ST-V2 | 2 | \$7.69 - AUD | \$15.38 - AUD | eBay.com.au | Other |
| Control Box | TB6560 Stepper Motor Driver | 6 | \$10.29 - AUD | \$61.74 - AUD | eBay.com.au | Other |
| Control Box | L298N Dual H-bridge | 1 | \$2.71 - AUD | \$2.71 - AUD | eBay.com.au | Other |
| Gantry Part I/ Gantry Part II/ Powder Bed | 26 Ncm Bipolar Stepper Motor | 3 | \$11.37 - AUD | \$34.11 - AUD | omc-stepperonline.com | Metal |
| Powder Bed | 59 Ncm Bipolar Stepper Motor | 3 | \$17.31 - AUD | \$51.93 - AUD | omc-stepperonline.com | Metal |
| Powder Bed | 12 VDC 20 RPM Gear Motor | 1 | \$16.99 - AUD | \$16.99 - AUD | eBay.com.au | Metal |

(continued)

| Designator | Component | Number | Cost per unit - currency | Total cost - currency | Source of materials | Material type |
|---|--|------------------------------------|---------------------------|-----------------------|---|---------------|
| Powder Bed | Berne REX-C-100 PID Temperature Controller | 1 | \$24.59 - AUD | \$24.59 - AUD | eBay.com.au | Other |
| Powder Bed | K-type Thermocouple | 1 | | | Included with Temperature Controller | Metal |
| Powder Bed | Fotek 40 A Solid State Relay | 1 | | | Included with Temperature Controller | Other |
| Powder Bed | 200 W Ceramic Heater | 2 | \$10.77 - AUD | \$21.54 - AUD | eBay.com.au | Composite |
| Control Box | DB25 Male-to-Female 1.5 m Cable | 2 | \$4.27 - AUD | \$8.54 - AUD | eBay.com.au | Other |
| Control Box | AWG18 PVC Multi-strand Copper Wire | 20 m | \$0.54/m - AUD | \$10.80 - AUD | Jaycar Electronics (Booval, QLD, Australia) | Composite |
| Powder Bed | 10 A Silicon Wire | 2 m | \$6.23/m - AUD | \$12.46 - AUD | Jaycar Electronics (Booval, QLD, Australia) | Composite |
| Control Box | 20 cm Male-to-Male Jumpers | 3 × 40pcs | \$1.63 - AUD | \$4.89 - AUD | eBay.com.au | Composite |
| Powder Bed | GX-16 2 Pin Plug + Socket | 1 | \$1.72 - AUD | \$1.72 - AUD | eBay.com.au | Metal |
| Powder Bed | GX-16 4 Pin Plug + Socket | 4 | \$1.72 - AUD | \$6.88 - AUD | eBay.com.au | Metal |
| Powder Bed | 500 mm Cable Chain (7 mm × 7 mm) | 1 | \$10.88 - AUD | \$10.88 - AUD | eBay.com.au | Polymer |
| Powder Bed | Ø = 10 mm Split Loom Tube | 1 m | \$2.50 - AUD | \$2.50 - AUD | Jaycar Electronics (Booval, QLD, Australia) | Polymer |
| Control Box | Steel Box (W = 0.5 m, D = 0.35 m, H = 0.1 m) | 1 | | | Recycled Computer Case | Metal |
| Mechanical Components | | | | | | |
| Powder Bed | Ø = 17 mm (W = 225 mm) Rubber Coated Roller | 1 | | | Recycled from Laser Printer | Composite |
| Gantry Part II/ Powder Bed | GT2 Timing Belt | 1 @ 180 mm, 1 @ 700 mm, 1 @ 880 mm | \$6.49 (2 m length) - AUD | \$6.49 - AUD | eBay.com.au | Polymer |
| Gantry Part II | GT2 Timing Belt Clamp | 2 | \$1.40 - AUD | \$1.40 - AUD | eBay.com.au | Metal |
| Gantry Part I/ Gantry Part II/ Powder Bed | 16 T GT2 Timing Pulley | 3 | \$1.29 - AUD | \$3.87 - AUD | eBay.com.au | Metal |
| Gantry Part I/ | 16 T GT2 Idler | 3 | \$1.54 - AUD | \$4.62 - AUD | eBay.com.au | Metal |

(continued on next page)

(continued)

| Designator | Component | Number | Cost per unit - currency | Total cost - currency | Source of materials | Material type |
|----------------------------------|--|------------------------|--|-----------------------|---|---------------|
| Gantry Part II/ Powder Bed | Pulley | | | | | |
| Powder Bed | Ø = 5 mm to 10 mm Shaft Coupling | 3 | \$1.88 - AUD | \$5.64 - AUD | eBay.com.au | Metal |
| Powder Bed | Ø = 6.35 to 8 mm Shaft Coupling | 1 | \$1.90 - AUD | \$1.90 - AUD | eBay.com.au | Metal |
| Powder Bed | Ø = 10 mm Trapezoidal Lead Screws + Brass Nuts | 3 @ 150 mm | \$13.26 - AUD | \$39.78 - AUD | eBay.com.au | Metal |
| Gantry Part II | Ø = 6 mm Linear Rail | 2 @ 200 mm | \$11.76 (400 mm) - AUD | \$11.76 - AUD | eBay.com.au | Metal |
| Gantry Part I | Ø = 10 mm Linear Rail | 2 @ 500 mm | \$13.06 - AUD | \$26.12 - AUD | eBay.com.au | Metal |
| Powder Bed | Ø = 12 mm Linear Rail | 2 @ 500 mm, 6 @ 200 mm | \$14.61 (500 mm), \$11.91 (400 mm) - AUD | \$64.95 - AUD | eBay.com.au | Metal |
| Gantry Part II | Ø = 6 mm Linear Rail Support | 4 | \$18.08 (4 pcs) - AUD | \$18.08 - AUD | eBay.com.au | Metal |
| Gantry Part I | Ø = 10 mm Linear Rail End Support | 4 | \$3.12 (2 pcs) - AUD | \$6.24 - AUD | eBay.com.au | Metal |
| Powder Bed | Ø = 12 mm Linear Rail Support | 4 | \$3.12 (2 pcs) - AUD | \$6.24 - AUD | eBay.com.au | Metal |
| Powder Bed | Ø = 12 mm Linear Rail End Support | 12 | \$3.12 (2 pcs) - AUD | \$18.72 - AUD | eBay.com.au | Metal |
| Gantry Part II | Ø = 6 mm Linear Bearing – Short | 4 | \$10.92 (2 pcs) - AUD | \$21.84 - AUD | eBay.com.au | Metal |
| Powder Bed | Ø = 8 mm Swivel Bearing | 2 | \$1.10 - AUD | \$2.20 - AUD | eBay.com.au | Metal |
| Gantry Part II | Ø = 10 mm Linear Bearing – Short | 2 | \$13.49 (2 pcs) - AUD | \$13.49 - AUD | eBay.com.au | Metal |
| Gantry Part II | Ø = 10 mm Linear Bearing – Long | 2 | \$21.04 (2 pcs) - AUD | \$21.04 - AUD | eBay.com.au | Metal |
| Powder Bed | Ø = 12 mm Linear Bearing – Short | 8 | \$14.03 (2 pcs) - AUD | \$56.12 - AUD | eBay.com.au | Metal |
| Materials | | | | | | |
| Powder Bed | Cork Sheet (H = 94 mm, W = 94 mm, TH = 6 mm) | 4 | \$13.90 (6 pcs) - AUD | \$13.90 - AUD | Bunnings Warehouse (Bundamba, QLD, Australia) | Other |
| Powder Bed | Copper Plate (H = 94 mm, W = 94 mm, TH = 3 mm) | 1 | \$19.95 - AUD | \$19.95 - AUD | Primary Metals & Alloys (Carole Park, QLD, Australia) | Metal |
| Powder Bed | Aluminium Plate (H = 94 mm, W = 94 mm, 6 mm) | 8 | \$32.00 - AUD | \$32.00 - AUD | Aluminium Warehouse (Yamanto, QLD, Australia) | Metal |
| Gantry Part I/ Gantry Part II | Aluminium Flat Bar (W = 100 mm, | 1 @ 506 mm, 1 | \$7.50 - AUD | \$7.50 - AUD | Aluminium Warehouse | Metal |

(continued)

| Designator | Component | Number | Cost per unit - currency | Total cost - currency | Source of materials | Material type |
|----------------------------------|--|-----------------------------------|--------------------------|-----------------------|---|---------------|
| | TH = 3 mm) | @ 260 | | | (Yamanto, QLD, Australia) | |
| Gantry Part II | Aluminium Angle (H = 30 mm, W = 30 mm, TH = 1.6 mm) | 1 @ 100 mm | \$2.20 - AUD | \$2.20 - AUD | Aluminium Warehouse (Yamanto, QLD, Australia) | Metal |
| Gantry Part II | Aluminium Angle (H = 40 mm, W = 25 mm, TH = 1.6 mm) | 2 @ 30 mm | \$1.80 - AUD | \$1.80 - AUD | Aluminium Warehouse (Yamanto, QLD, Australia) | Metal |
| Gantry Part I | Aluminium Angle (H = 75 mm, W = 75 mm, TH = 3 mm) | 2 @ 285 mm | \$9.00 - AUD | \$9.00 AUD | Aluminium Warehouse (Yamanto, QLD, Australia) | Metal |
| Powder Bed | Aluminium Angle (H = 75 mm, W = 25 mm, TH = 1.6 mm) | 1 @ 40 mm, 1 @ 312 mm, 4 @ 400 mm | \$28.00 - AUD | \$28.00 - AUD | Aluminium Warehouse (Yamanto, QLD, Australia) | Metal |
| Gantry Part I | Aluminium Angle (H = 125 mm, W = 50 mm, TH = 3 mm) | 2 @ 550 mm | \$44.00 - AUD | \$44.00 - AUD | Aluminium Warehouse (Yamanto, QLD, Australia) | Metal |
| Powder Bed | Aluminium Box (H = 40 mm, W = 40 mm, TH = 1.6 mm) | 2 @ 100 mm | \$7.50 - AUD | \$7.50 - AUD | Aluminium Warehouse (Yamanto, QLD, Australia) | Metal |
| Gantry Part I | Aluminium Box (H = 25 mm, W = 50 mm, TH = 3 mm) | 2 @ 510 mm | \$12.00 - AUD | \$12.00 - AUD | Aluminium Warehouse (Yamanto, QLD, Australia) | Metal |
| Powder Bed | Aluminium Box (H = 100 mm, W = 100 mm, TH = 3 mm) | 3 @ 200 mm | \$44.00 - AUD | \$44.00 - AUD | Aluminium Warehouse (Yamanto, QLD, Australia) | Metal |
| Powder Bed | Aluminium C-section (H = 65 mm, W = 150 mm, TH = 6 mm) | 2 @ 500 mm | \$55.00 - AUD | \$55.00 - AUD | Aluminium Warehouse (Yamanto, QLD, Australia) | Metal |
| Hardware | | | | | | |
| Gantry Part I/ Gantry Part II | M3 SS Nylon Lock Nut | 12 | \$1.47 (10 pcs) - AUD | \$2.94 - AUD | Nutz & Boltz (Raceview, QLD, Australia) | Composite |
| Gantry Part I/ Gantry Part II | M3 SS Flat Washer | 12 | \$2.75 (100 pcs) - AUD | \$2.75 - AUD | Nutz & Boltz (Raceview, QLD, Australia) | Metal |
| Powder Bed | M3 × 20 mm Brass Stand Off | 4 | \$2.86 - AUD | \$11.44 - AUD | eBay.com.au | Metal |
| Powder Bed | M3 × 6 mm SS Socket Head Bolt | 4 | \$1.47 (10 pcs) - AUD | \$1.47 - AUD | Nutz & Boltz (Raceview, QLD, Australia) | Metal |
| Gantry Part I/ Gantry Part II | M3 × 8 mm SS Socket Head Bolt | 10 | \$1.47 (10 pcs) - AUD | \$1.47 - AUD | Nutz & Boltz (Raceview, QLD, Australia) | Metal |

(continued on next page)

(continued)

| Designator | Component | Number | Cost per unit - currency | Total cost - currency | Source of materials | Material type |
|---|--------------------------------|------------|--------------------------|-----------------------|---|---------------|
| Powder Bed | M3 × 12 mm SS Countersunk Bolt | 8 | \$1.83 (10 pcs) - AUD | \$1.83 - AUD | Nutz & Boltz (Raceview, QLD, Australia) | Metal |
| Gantry Part II | M3 × 16 mm SS Socket Head Bolt | 8 | \$1.83 (10 pcs) - AUD | \$1.83 - AUD | Nutz & Boltz (Raceview, QLD, Australia) | Metal |
| Powder Bed | M3 × 25 mm Socket Head Bolt | 8 | \$2.20 (10 pcs) - AUD | \$2.20 - AUD | Nutz & Boltz (Raceview, QLD, Australia) | Metal |
| Gantry Part I/ Gantry Part II/ Powder Bed | M4 SS Nylon Lock Nut | 50 | \$1.47 (10 pcs) - AUD | \$7.35 - AUD | Nutz & Boltz (Raceview, QLD, Australia) | Composite |
| Gantry Part I | M4 × 12 mm SS Socket Head Bolt | 12 | \$1.83 (10 pcs) - AUD | \$3.66 - AUD | Nutz & Boltz (Raceview, QLD, Australia) | Metal |
| Gantry Part II | M4 × 12 mm SS Countersunk Bolt | 8 | \$1.83 (10 pcs) - AUD | \$1.83 - AUD | Nutz & Boltz (Raceview, QLD, Australia) | Metal |
| Gantry Part II/ Powder Bed | M4 × 20 mm SS Socket Head Bolt | 42 | \$1.83 (10 pcs) - AUD | \$9.15 - AUD | Nutz & Boltz (Raceview, QLD, Australia) | Metal |
| Gantry Part I/ Gantry Part II/ Powder Bed | M5 SS Nylon Lock Nut | 38 | \$1.47 (10 pcs) - AUD | \$5.88 - AUD | Nutz & Boltz (Raceview, QLD, Australia) | Composite |
| Gantry Part I/ Gantry Part II/ Powder Bed | M5 SS Flat Washer | 6 | \$2.75 (100 pcs) - AUD | \$2.75 - AUD | Nutz & Boltz (Raceview, QLD, Australia) | Metal |
| Gantry Part I | M5 × 25 mm SS Socket Head Bolt | 8 | \$2.93 (10 pcs) - AUD | \$2.93 - AUD | Nutz & Boltz (Raceview, QLD, Australia) | Metal |
| Powder Bed | M5 × 25 mm SS Hex Head Bolt | 24 | \$2.45 (10 pcs) - AUD | \$7.35 - AUD | Nutz & Boltz (Raceview, QLD, Australia) | Metal |
| Gantry Part I/ Gantry Part II/ Powder Bed | M5 × 35 mm Socket Head Bolt | 3 | \$3.48 (10 pcs) - AUD | \$3.48 - AUD | Nutz & Boltz (Raceview, QLD, Australia) | Metal |
| Powder Bed | M8 Galvanized Nuts | 4 | \$0.17 - AUD | \$0.68 - AUD | Bunnings Warehouse (Bundamba, QLD, Australia) | Metal |
| Powder Bed | M8 Galvanized Threaded Rod | 2 @ 230 mm | \$5.50 - AUD | \$5.50 - AUD | Bunnings Warehouse (Bundamba, QLD, Australia) | Metal |
| Total | | | | \$1,162.32 - AUD | | |

Legend: Ø – diameter; SS – stainless steel; H – height; W – width; TH – wall thickness

NOTE: All prices are in Australian dollars (AUD) and inclusive of the 10% Goods and Services Tax.

5. Build instructions

This section describes the fabrication and assembly of each part of the SLS machine. The tools required for fabrication and assembly are found in most laboratory spaces and workshops with the exception of an end mill. It is not an absolute necessity to use an end mill to cut all of the holes in the aluminium as a drill press and an angle grinder could perform the same

actions. However, as this would increase fabrication time and potentially lead to inaccuracies in the final product, the use of an end mill is highly recommended.

5.1. Gantry Part I

The fabrication and assembly of the gantry is broken into two sections (I & II) to avoid confusion between parts which make up the X and Y axes. To begin, use an end mill or drill to make all attachment holes in the aluminium sections for Gantry Part I (Figs. 7 & 8) according to the supplied CAD files.

- 1) Use four M4x25 mm bolts to attach the 75x75 mm aluminium angle sections (B) to the top of the 25x50 mm aluminium box sections (A).
- 2) Attach the 25x125 mm aluminium angle sections (C) to the inside of the 75x75 mm aluminium angle sections (B) perpendicular to the base with four M4x25 mm bolts. Use a set square to ensure that the angle between them is as close to 90° as possible so that the laser remains the same distance from the powder bed as it traverses.
- 3) Using four M4x25 mm bolts, attach the 100 mm aluminium flat bar (D) to the uprights (C).
- 4) Fit the 10 mm linear rail end supports to the inside of the uprights (C) using eight M5x25 mm bolts.

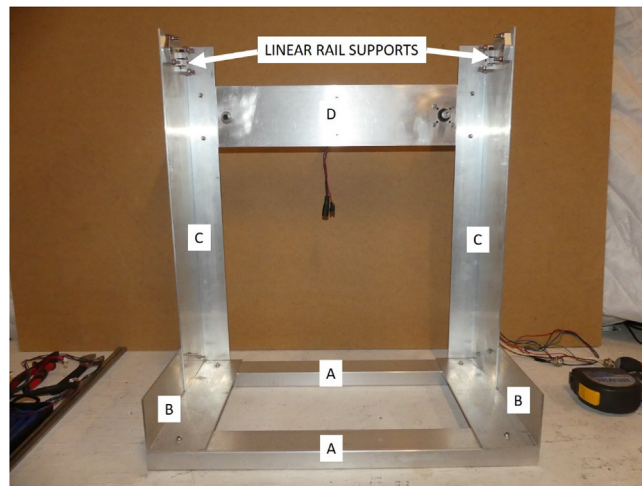


Fig. 7. Gantry Part I (front view).

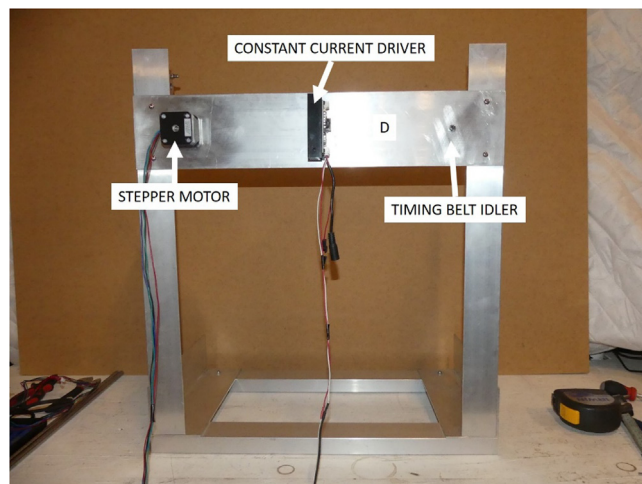


Fig. 8. Gantry Part I (rear view).

- 5) Mount a 26 Ncm stepper motor to the 100 mm aluminium flat bar (D) using four M3x8 mm bolts with the shaft facing towards the front of the machine. Then place a 16 T T2 timing pulley on the shaft of the stepper motor and tighten the grub screw.
- 6) Using an M5x35 socket head bolt, two M5 flat washers and two M5 nylon locking nuts, mount a T2 idler pulley to the 100 mm aluminium flat bar (D). Ensure that the idler pulley is in line with the pulley on the stepper motor.
- 7) Attach the laser's constant current driver to the rear of the 100 mm aluminium flat bar using two M3x8 mm bolts and M3 flat washers.

5.2. Gantry Part II

Use a drill or end mill to make all attachment holes in the aluminium sections for Gantry Part II (Figs. 9, 10, 11 & 12) according to the supplied CAD file.

- 1) Attach the four 6 mm linear bearings back-to-back onto the 25x25 mm aluminium angle section (F) using eight M3x16 mm bolts and M3 nylon locking nuts.
- 2) Insert the 6 mm linear rails into the 6 mm linear bearings whilst being careful not to damage the ball races inside. Attach these 6 mm linear rails to the 100 mm aluminium flat bar (E) using four 6 mm linear rail end mounts and eight M4x12 mm countersunk bolts and M4 nylon locking nuts.

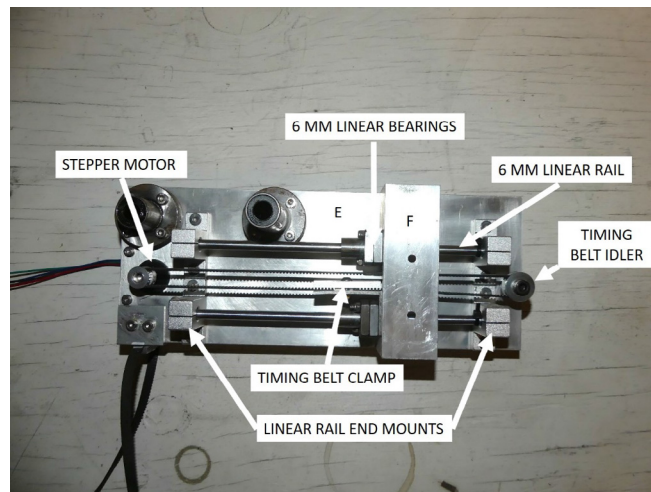


Fig. 9. Gantry Part II (front view).

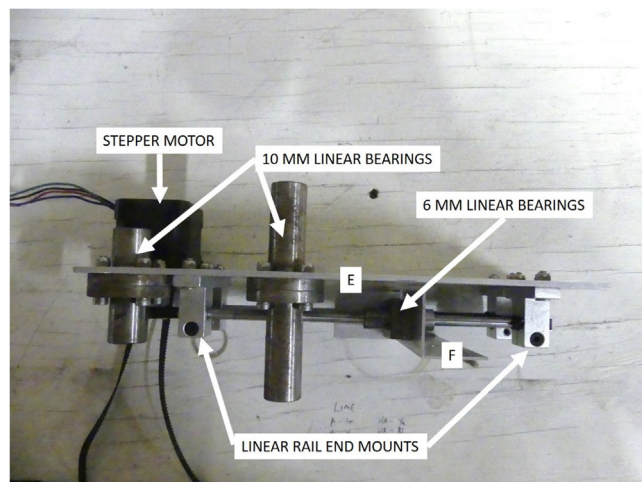


Fig. 10. Gantry Part II (top view).

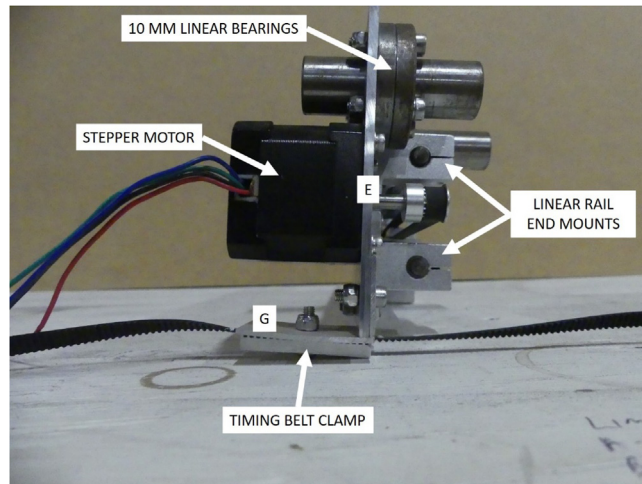


Fig. 11. Gantry Part II (side view).

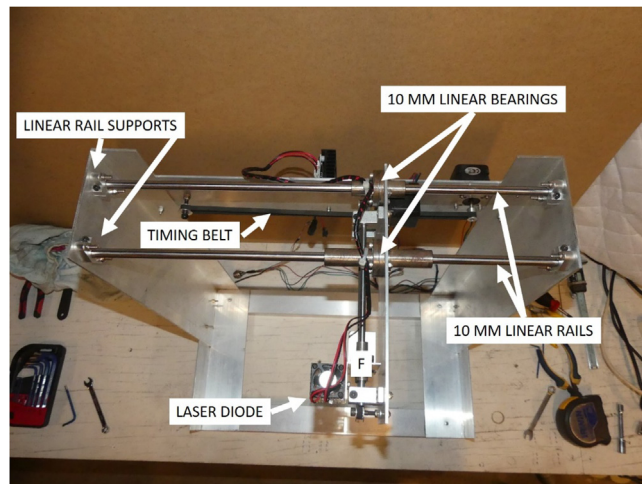


Fig. 12. Gantry Part II attached to Gantry Part I (top view).

- 3) Attach a 26 Ncm stepper motor, 16 T T2 pulley and idler pulley to the 100 mm aluminium flat bar (E) ensuring that the idler pulley is aligned with the pulley on the stepper motor.
- 4) Feed the 180 mm long T2 timing belt around the stepper motor and idler pulleys and while tensioned, clamp to the 25x25 mm aluminium angle section using a timing belt clamp, an M4x20 mm bolt and M4 nylon locking nut.
- 5) Mount the 10 mm linear bearings (short to the left and long to the right) back-to-back to the 100 mm aluminium flat bar (E) using eight M4x20 mm bolts and M4 nylon locking nuts.
- 6) Using a timing belt clamp, an M4x20 mm bolt and M4 nylon locking nut, attach the 700 mm long T2 timing belt to a 25x40 mm aluminium right angle section (G). Then, using two M4x20 mm bolts and M4 nylon locking nuts, attach the 25x40 mm aluminium right angle section (G) to the 100 mm aluminium flat bar (E).
- 7) Attach Gantry Part II to Gantry Part I by inserting the 10 mm linear rails into the bearings then clamping them inside the linear rail supports by tightening the grub screws. Ensure that Gantry Part II slides freely from one end to the other. If there is any resistance, adjust the alignment of the 10 mm linear rails in relation to each other by tweaking the position of the linear rail supports.
- 8) Feed the 700 mm T2 timing belt around the stepper motor and idler pulleys which are mounted on the 100 mm aluminium flat bar (D).
- 9) Mount the laser diode module to the 25x25 mm aluminium angle section (F) using two M3x8 mm bolts and M3 flat washers. Use a set square or level to ensure the laser module is mounted at an angle of 90° relative to the gantry base.
- 10) Using cable ties, attach the wires for the laser module to the 10 mm linear bearings allowing for some slack to account for movement of the laser.

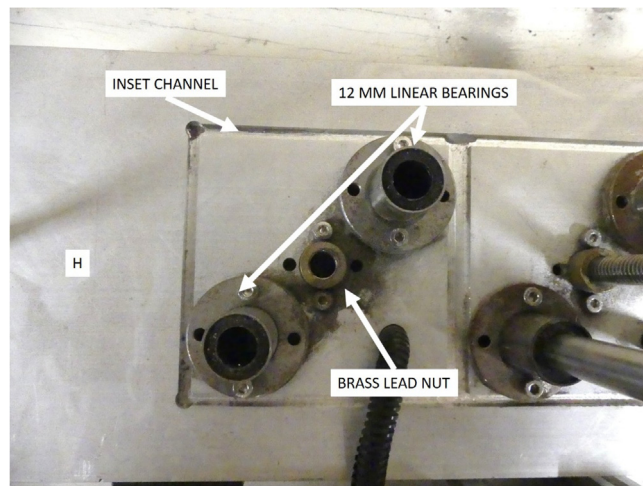


Fig. 13. Lower section of the powder bed (top view).

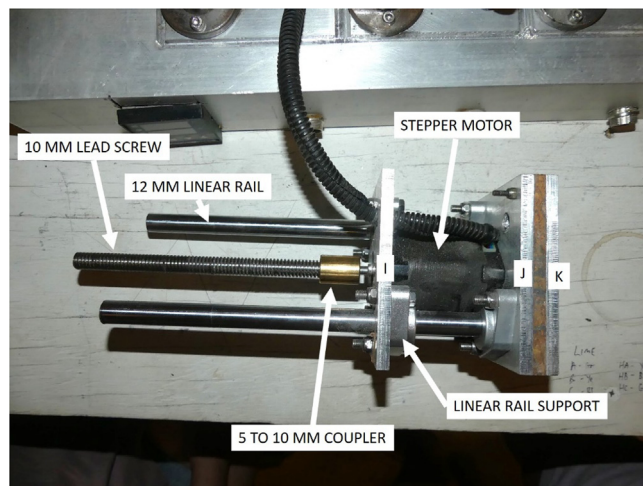


Fig. 14. Feed piston (side view).

5.3. Powder Bed

The following section describes the fabrication and assembly of the powder bed inclusive of the recoater mechanism (Figs. 13 - 23). If an end mill is not available, this section will require several parts to be slightly modified to cater for the use of different tools. Suggestions of the modifications will be made, however specific details (such as images) are not available as this machine was constructed from end milled parts.

- 1) Use an end mill to machine the inset channels (Fig. 13) which are used to locate the pistons into the top of the powder bed's lower section (H, 65x150 mm aluminium c-section). The dimensions for this can be found in the supplied CAD file. If an end mill is not available, it is suggested to attach (glue or bolt) locaters in the same position so that the piston sleeves remain centrally located during assembly.
- 2) Attach all six 12 mm linear bearings to the top of the lower section of the powder bed (H) as shown in Fig. 13. Use M4x20 mm bolts with M4 nylon locking nuts as fixings.
- 3) Mount a 59 Ncm stepper motor to the 94x94 mm aluminium plate (I) using four M3x8 mm bolts, then attach a 10 mm lead screw to the stepper motor's shaft using a 5 to 10 mm shaft coupler.
- 4) Attach the two 94x94 mm aluminium plates (I & J) together by bolting the linear rail supports to two corners of each plate, then slide the 12 mm linear rails inside the linear rail supports until the upper 94x94 mm aluminium plate (J) is firmly against the stepper motor. Proceed to tighten the grub screws in each of the linear rail supports.

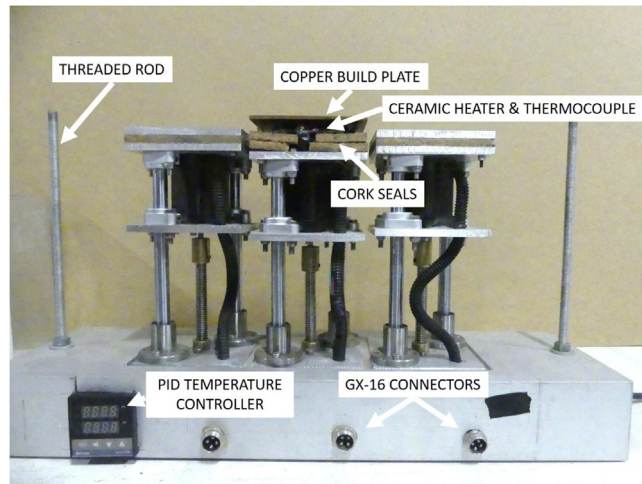


Fig. 15. Powder bed with piston sleeves removed (front view).

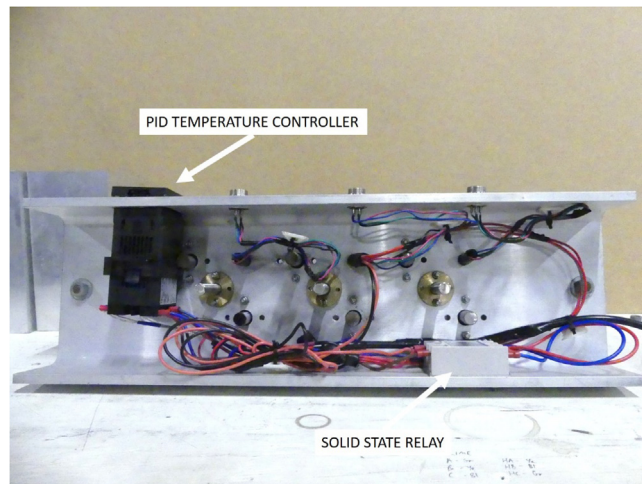


Fig. 16. Powder bed (bottom view).

- 5) Attach the upper 94x94 mm aluminium plates (J & K) to each other using M3x25 mm bolts and M3 nylon locking nuts with a 94x94 mm cork spacer in between. Tighten until firm, over tightening may result in bending of the aluminium plate.
- 6) Repeat for the other two pistons with the exception of the build piston (center). For this piston, the upper 94x94 mm plate is copper and the two ceramic heaters and thermocouple are placed between the 94x94 mm cork spacers and the copper plate.
- 7) To mount each piston to the lower section of the powder bed (H), screw the lead screw of each piston into the corresponding brass nut while aligning the 12 mm linear rails with the linear bearings. Screw the lead screw into the brass nut until the linear rails are visible from the underside of the assembly.
- 8) Attach the lengths of M8 threaded rod to the outer edges of the lower section of the powder bed (H) using two M8 nuts and flat washers.
- 9) Using a die grinder (or similar tool) cut a hole in the front of the powder bed base to mount the PID temperature controller. Mount the solid state relay using two M4x20 mm bolts and nylon locking nuts in the position shown in Fig. 16.
- 10) Connect the PID controller, solid state relay, thermocouple and 240 VAC power source according to the circuit diagram in Fig. 17. All connections should be insulated using appropriately rated heat shrink sleeving. The AC system should then be inspected and certified by qualified personnel.
- 11) Attach the geared DC motor to one side (outside) of the 40x40 mm aluminium box section (L) using four M3x6 mm socket head bolts. Mount an 8 mm bore swivel bearing to the inside of the box section using two M4x20 mm socket head bolts and nylon locking nuts.

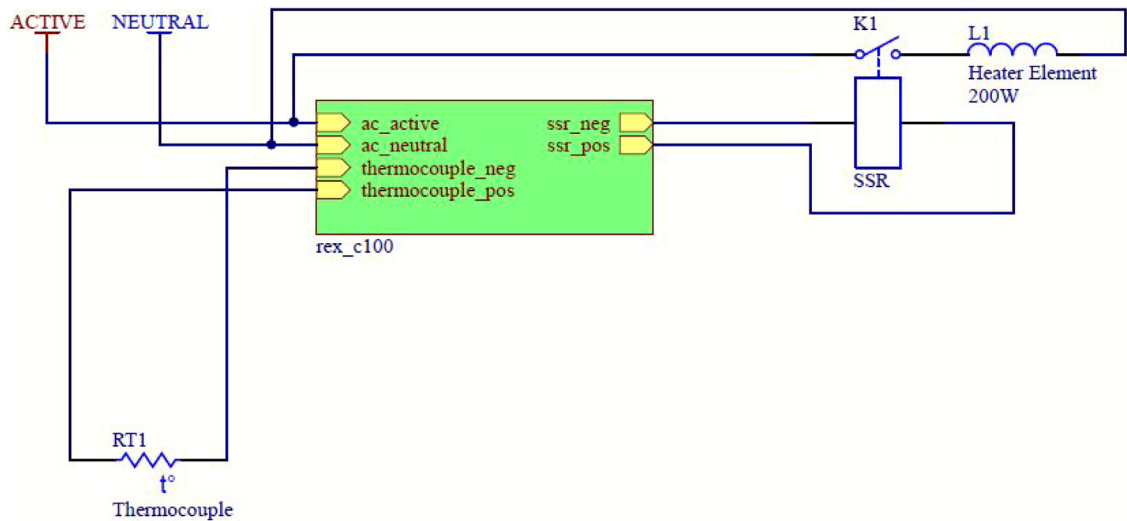


Fig. 17. Wiring schematic for the powder bed heating system.

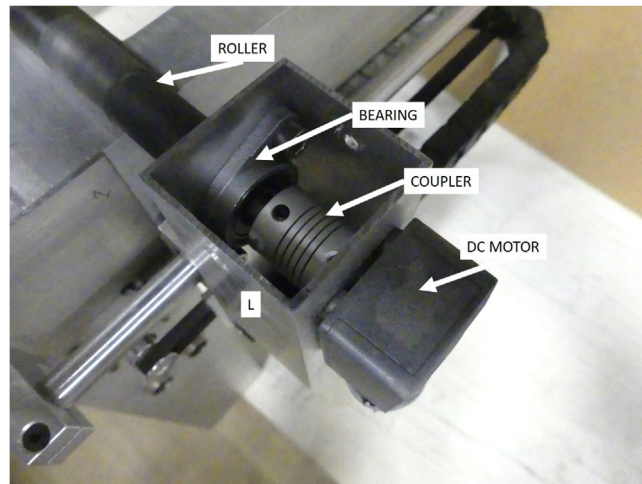


Fig. 18. Recoater assembly (driven end).

- 12) Mate the rubber coated roller to the motor shaft using the 6.35 to 8 mm shaft coupler and tighten the grub screws.
- 13) Mount the other 8 mm bore swivel bearing to the inside of the other 40x40 mm aluminium box section (M) using two M4x20 mm socket head bolts and nylon locking nuts.
- 14) Mount a 12 mm linear bearing to each 40x40 aluminium box section (L & M) using four M4x14 mm socket head bolts for each.
- 15) Attach all four lengths of 75x25 mm aluminium angle (O, P, Q & R) to each corner of the machined aluminium 65x150 mm c-section top plate (N) at each corner. To attach each corner, insert two M5x25 mm socket head bolts through a 12 mm linear rail support, then through the holes in the aluminium angle and c-section and fix using nylon locking nuts.
- 16) Attach a 26 Ncm stepper motor to the inside of the front left length of aluminium angle (O) along with the 20 tooth GT2 pulley. Mount the idler pulley to the aluminium angle opposite (R) using an M5x35 mm mild steel bolt and two nylon locking nuts.
- 17) Combine the recoater assembly and the top plate by feeding the 12 mm linear rails through the linear bearings and rail supports.
- 18) To improve the rigidity of the recoater assembly, attach the remaining length of 75x25 mm aluminium angle (S) to the 40x40 mm box sections (L & M) using two M4x20 mm socket head bolts and nylon locking nuts.

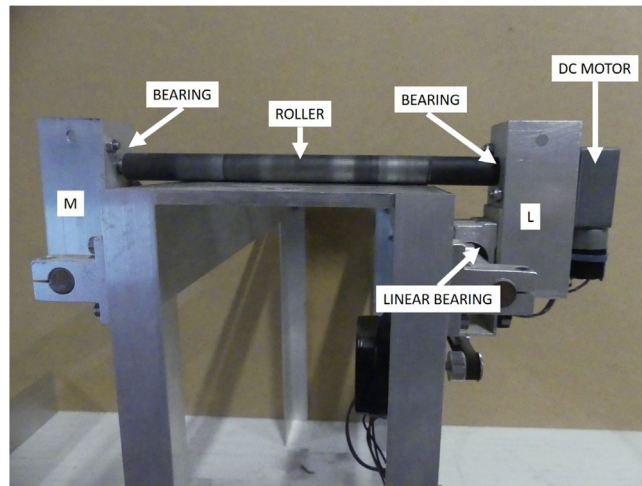


Fig. 19. Recoater assembly (side view).

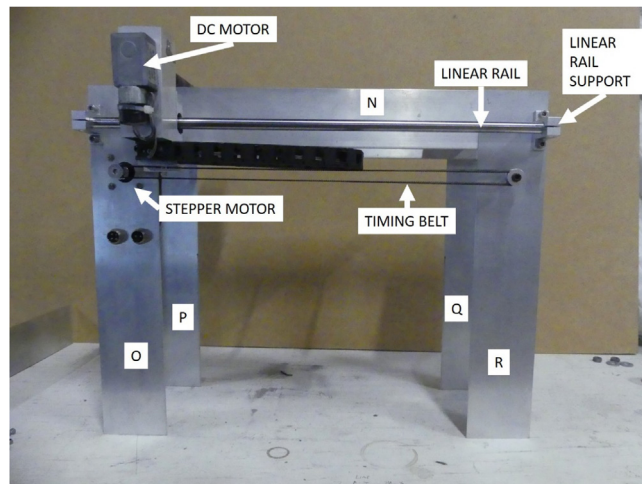


Fig. 20. Recoater assembly and upper powder bed section (front view).

- 19) Push each of the piston sleeves (100x100 mm aluminium box section) over each piston. Mate the lower and upper parts of the assembly by sliding the lower section into the underneath of the upper section. Fix the two sections together by placing two galvanized M8 washers and nuts on the threaded rod and tightening.
- 20) To finalize the assembly, place the powder bed inside the gantry. The fit should be very tight, however, if the powder bed has movement, fix the two pieces together using G-clamps or similar.

5.4. Control Electronics

This section describes the connection of the control box consisting of the parallel port isolation boards, motor drivers and power supply. Once assembled, the system should be inspected and certified by qualified personnel prior to operation.

- 1) Remove the cover of the control PC (ensuring the power is disconnected) and fit the parallel port expansion card (CH351Q) into a spare PCI slot. If the computer chosen runs an operating system newer than Windows XP, it is possible that two expansion cards may be necessary or the installation method may be different. Once the expansion card has been secured, replace the cover of the control PC.
- 2) Mount the two parallel port isolation boards, six stepper motor drivers, h-bridge and power supply inside the recycled computer case (or chosen variant) with adequate separation distance so that each of the screw terminals can be accessed.

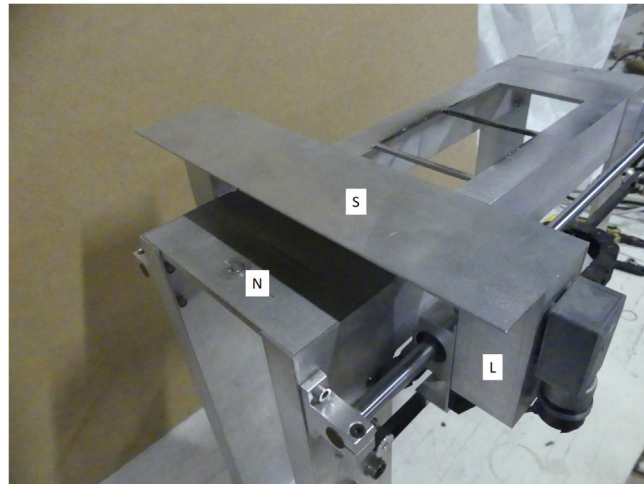


Fig. 21. Isometric view of the recoater assembly and top plate.

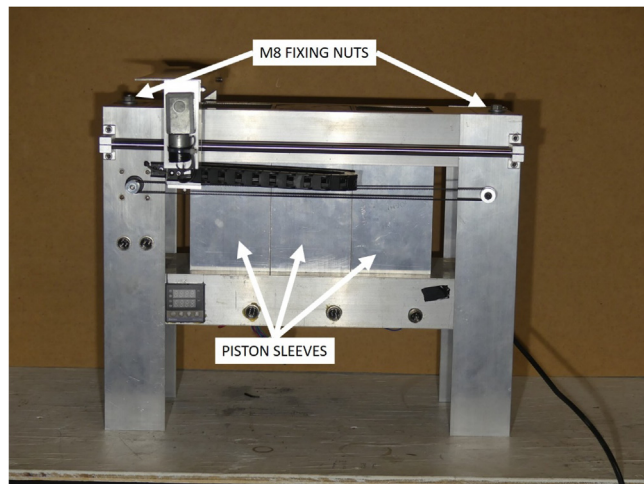


Fig. 22. Assembled powder bed.

- 3) Using the 20 cm male-to-male jumpers, connect the logic level components of the system together according to the schematic in Fig. 24. A larger format version of this figure can be found in the data repository associated with this document (system.jpg).
- 4) For each of the stepper motors, cut four 0.5 m lengths of 18 AWG wire and solder them to a 4 pin GX16 plug. Fix the other end of each wire into the screw terminals on each of the associated stepper motor driver boards.
- 5) To finalize the wiring, connect each of the GX16 motor plugs to their corresponding axes on the main body of the SLS machine and connect each of the parallel port interface cards to their corresponding parallel ports on the control PC using the DB25 cables.

5.5. Control software setup

The interface program chosen was Mach3 (Newfangled Solutions LLC, Livermore Falls, Maine, USA) which is a parallel port based CNC control suite popular among the hobbyist community. Mach3 converts a G-code instruction set into control signals based upon user-defined output parameters such as axis pin selection and motor movement profiles. The motor movement profiles are preset according to the physical properties of the stepper motors, belt drives and lead screws. Accordingly, this section describes the process of setting up the control software for the SLS machine.

- 1) Install the drivers for the PCI parallel port expansion card as per the instructions supplied with the device. Download and install the Mach3 CNC control software and begin a new profile.

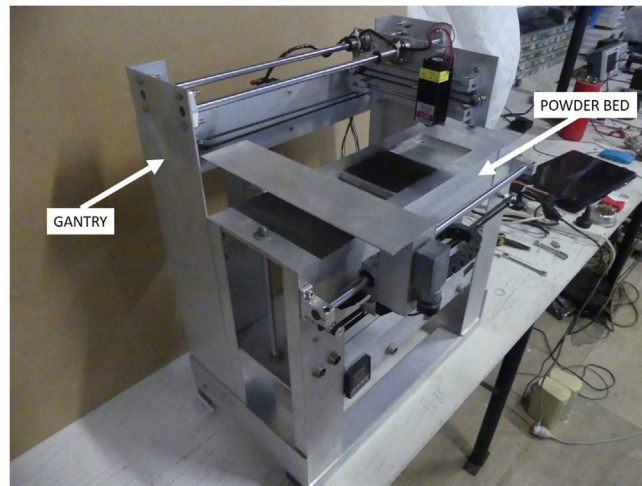


Fig. 23. SLS machine finalized assembly.

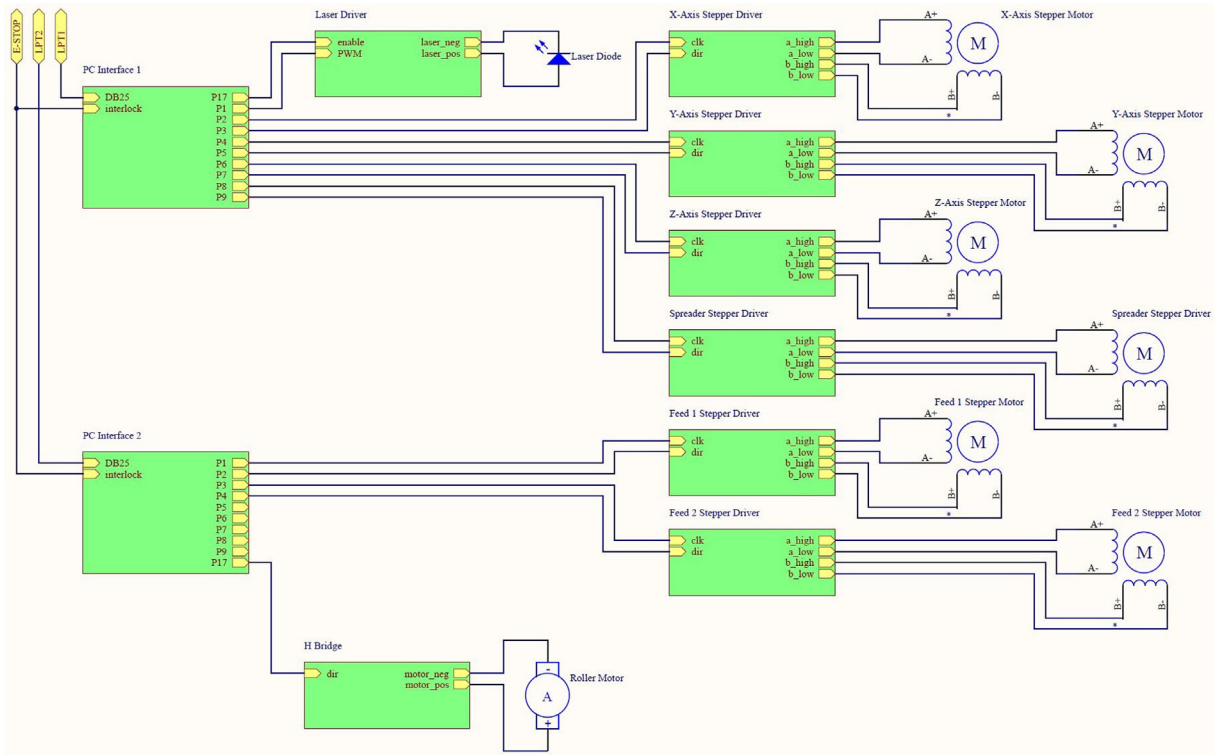


Fig. 24. Control box wiring diagram.

- 2) Open the dialog box “Ports and Pins” under the menu “Config”. Under the first tab enter the base addresses of each of the two parallel ports (Fig. 25). If unsure of the base addresses, they can be found under the port properties in device manager.
- 3) Select the next tab called “Motor Outputs” and enter all of the pin and port numbers as shown in Fig. 26. These are the designated pins that the stepper motor drivers are connected to in the control box.

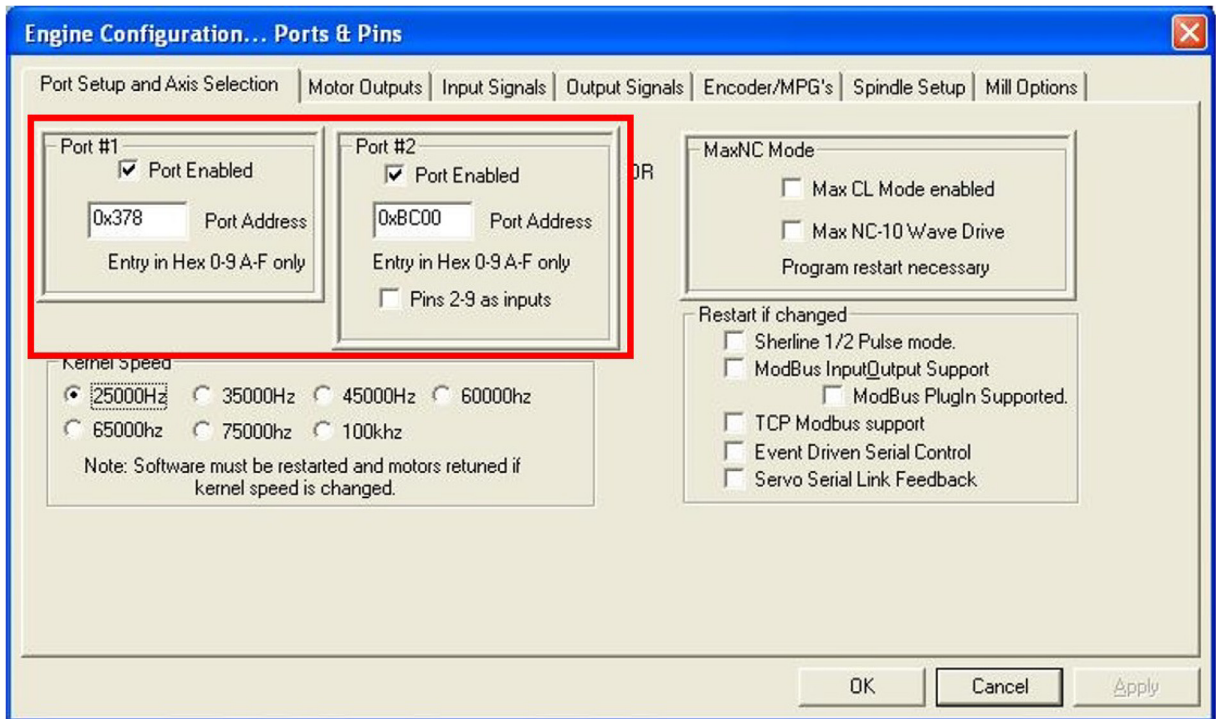


Fig. 25. Mach3 port setup and axis selection.

- 4) Select the tab called “Output Signals” and enable outputs #1, #2 and #3 while assigning the pins as shown in Fig. 27. Output #1 is the laser control pin while outputs #2 and #3 are the forward and reverse directions of the recoater roller.
- 5) Select the tab called “Spindle Setup” and set the relay control to switch on output #1 when an M3 or M4 command is executed. Set the mist (M7 command) and flood (M8 command) controls to turn on outputs #2 and #3 respectively. Check the box enabling PWM control of the spindle and set the base frequency to 1000 Hz while setting all of the spindle delays to zero (Fig. 28). Apply the changes made and close the dialog box.
- 6) Open the dialog box “Pulley Selection” under the menu “Config” and enter the maximum and minimum speeds as 100 and 0 respectively under “Pulley Number 1” (Fig. 29). These values represent the maximum and minimum values corresponding to the maximum and minimum PWM on output #1 for laser control.
- 7) Open the dialog box “Motor Tuning and Setup” under the menu “Config”. For each axis, set the steps per unit, velocity and acceleration values according to Table 1 and Fig. 30. The velocities, particularly the ones representing scan speed, can be adjusted in the G-code up to these maximum values.
- 1) Once this setup has been completed, the machine can be operated by the G-code commands described in Table 2.

5.6. Slicing software setup

Conversion of the 3D model into a G-code instruction set was performed by an open source program called Slic3r (Alessandro Ranellucci, Rome, Italy). Slic3r is based on the fused deposition modeling (FDM) process, however, most processing parameters were directly translatable to the SLS process with the appropriate settings. Accordingly, this section describes the setup procedure of Slic3r so that the G-code is output in a format that can be converted by the supplied MATLAB script.

- 1) Under the tab “Print Settings”, the following settings should be entered under their corresponding subsection:

- Layers and perimeters – the layer height and first layer height should be set to 0.1 mm. Vertical shells should be set to 1 and horizontal shells to 0.
- Infill – the fill density should be set to 100% in a rectilinear pattern which is filled every layer at an angle of 45°.
- Skirt and brim – the number of loops and brim width should both be set to 0.
- Support material – uncheck the generate support material box and set number of raft layers to 0.

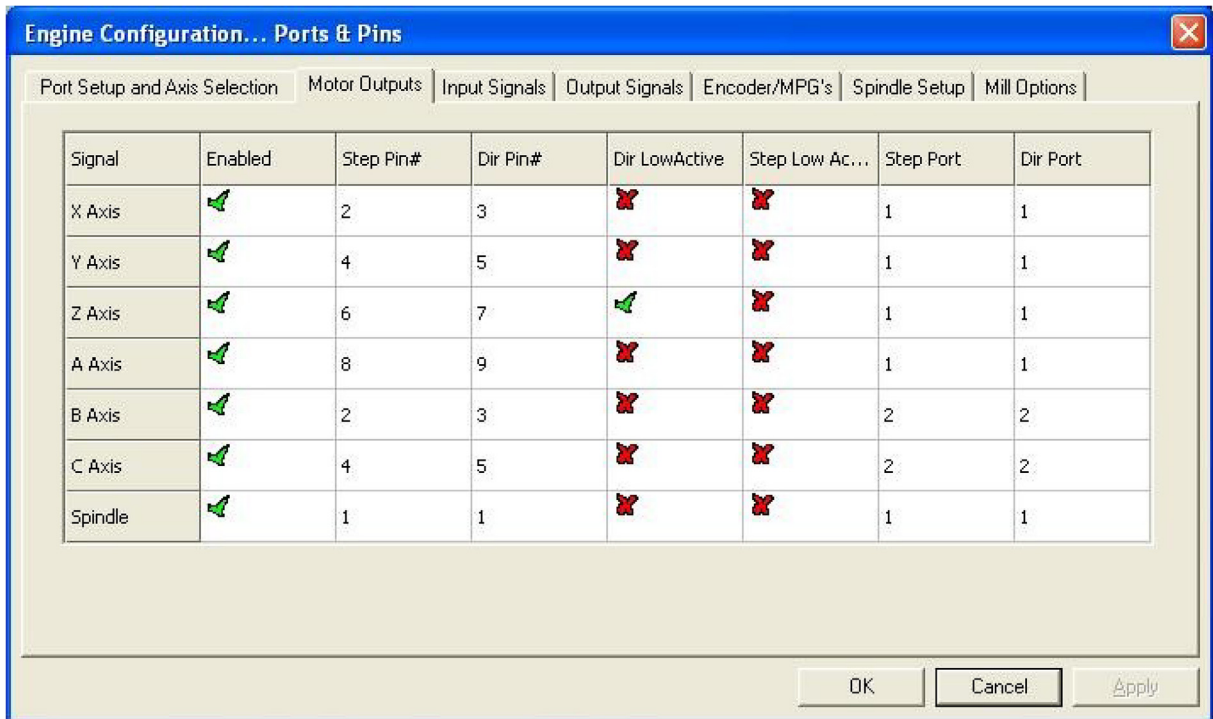


Fig. 26. Mach3 motor output setup.

2) Under the tab “Printer Settings”, the following settings should be entered under their corresponding subsection:

- General – set the bed shape according to Fig. 31.
- Custom G-code – add an M6 command after the layer change.
- Extruder 1 – set the nozzle diameter to 0.22 mm (this corresponds to the default scan spacing of 0.35 mm or 0% overlap of the laser spot).

The aforementioned Slic3r settings are the defaults which were used to process the polyamide-12 powder (Section 7), however, as this machine was intended for processing novel materials, it is likely that many of these parameters will require adjustment according to the user’s specific application requirements.

6. Operation instructions

The section describes the step-by-step operation of the SLS machine which will enable the user to produce parts using powdered polyamide-12 feedstock. NOTE: Laser safety glasses (of appropriate wavelength) and a lockable workspace are required for safe operation of this machine.

- 1) Select or create a 3D model using any desired CAD software and save the model as an .STL file.
- 2) Open Slic3r and add the model(s) to the workspace. Perform any orientation/translation movements of models and then export the G-code (Fig. 32).
- 3) Open the G-code post-processing script in MATLAB and set the laser power to 30%, scan speed to 1800 mm/min and enter the number of objects (models) that were placed in the workspace. Run the script with the input file as the G-code generated previously by Slic3r.
- 4) Open Mach3 and load the G-code that was generated by the MATLAB script.

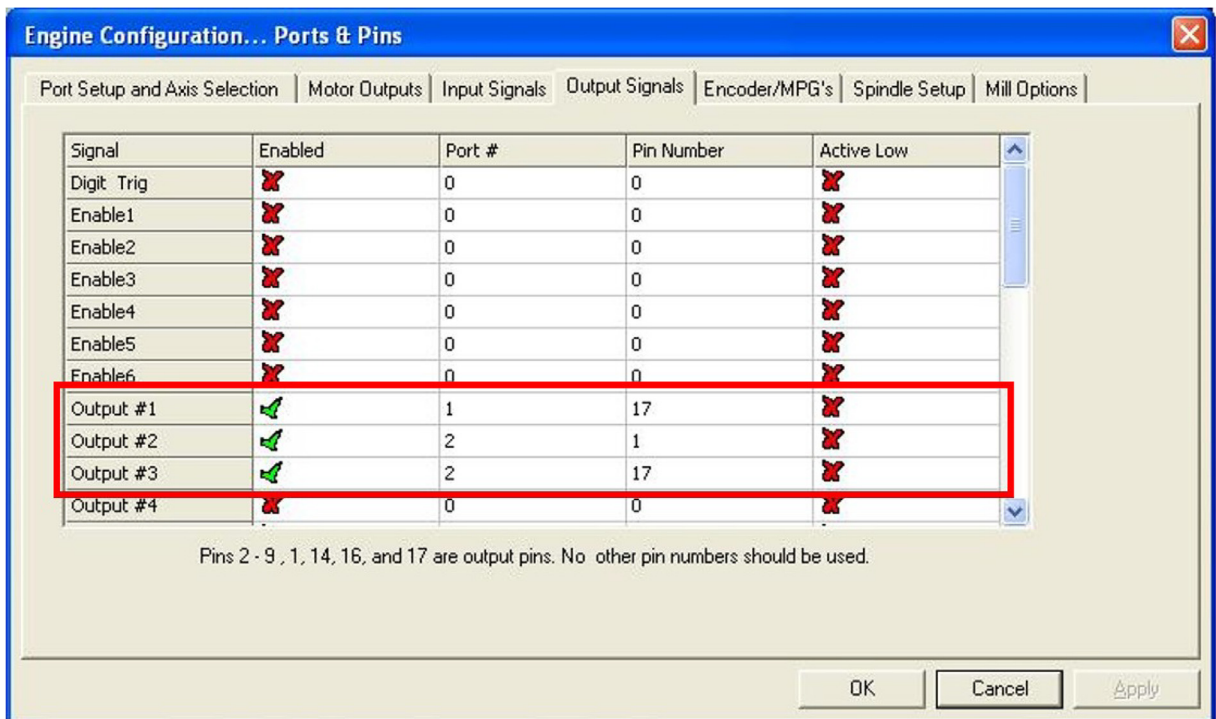


Fig. 27. Mach3 output signal designators.

- 5) Turn the power on for the SLS machine control box. Using the Mach3 console, actuate the feed pistons (axes B and C) in the downward direction by at least half of the height of the model being built. While placing a straight edge across the build piston (Fig. 33), actuate it in the upward direction at least 1 mm above the piston assembly then actuate it in the downward direction until the surface of the piston is level with the top of the piston assembly. This is done to account for any backlash in the lead screw.
- 6) Load the feed pistons to the top with polyamide-12 powder.
- 7) Turn the power on for the PID controller then set the temperature to 180 °C by pressing SET and then using the arrows to change the value. **From this moment on, care should be taken when touching the metal surfaces as they could be very hot.**
- 8) Put the laser safety glasses on and turn the power on for the laser module. **From this point onwards it is important that laser safety glasses are worn at all times to avoid eye damage – also ensure other people are isolated from any radiation – e.g. by locking the door.**
- 9) The build sequence can now be initiated by clicking “Cycle Start” on the Mach3 interface. For the first couple of operations, it is recommended that the build sequences are closely monitored to ensure that the machine has been set up correctly.
- 10) When the build has completed, the power to the heater and laser can be switched off and the build piston allowed to cool for at least 30 min.
- 11) Once the powder bed has had sufficient time to cool, the powder can be removed from the build piston and feed pistons using a small wet and dry vacuum cleaner. If the powder cake is to be re-used it is recommended that a new vacuum cleaner is purchased and dedicated to this job to avoid contamination.
- 12) Remove the part(s) using a paint scraper or similar (Fig. 34). Once the build volume is empty, use a rag and solvent (ethanol or similar) to wipe the build plate clean.

It is recommended that all of the moving parts are inspected periodically for wear and lubricated using a low viscosity grease.

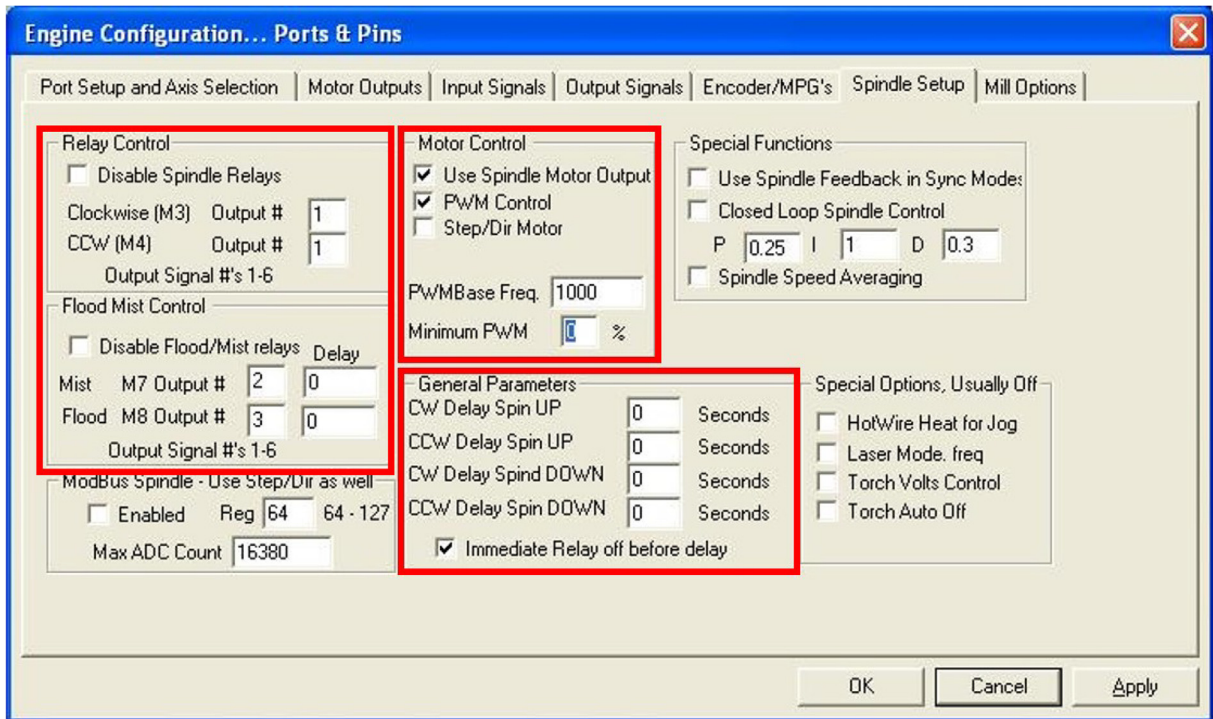


Fig. 28. Mach3 spindle setup.

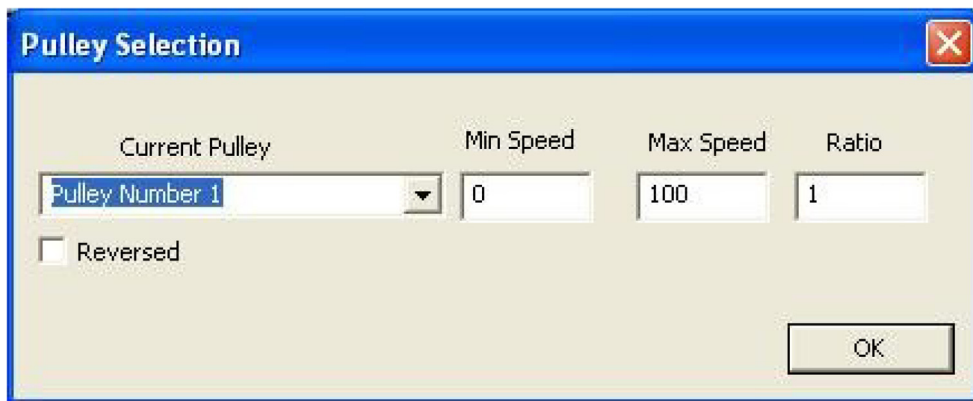


Fig. 29. Mach3 pulley selection.

Table 1
Motor movement profiles.

| Axis | Steps Per Millimeter | Velocity (mm/min) | Acceleration (mm/min ²) |
|-----------------------|----------------------|-------------------|-------------------------------------|
| X | 50 | 3000 | 2500 |
| Y | 50 | 3000 | 2500 |
| Z (build piston) | 100 | 50 | 50 |
| A (recoater) | 100 | 75 | 200 |
| B (left feed piston) | 100 | 50 | 50 |
| C (right feed piston) | 100 | 50 | 50 |

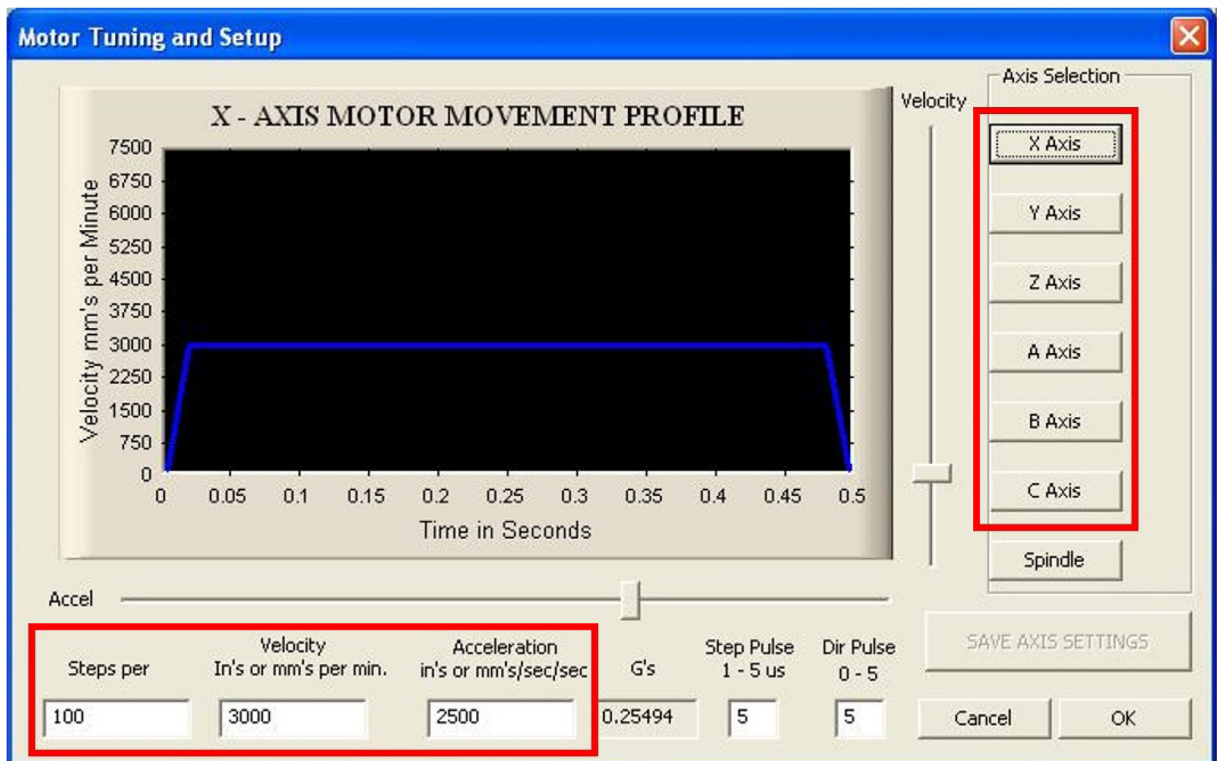


Fig. 30. Mach3 motor tuning and setup.

Table 2
G-code instructions used to control the SLS machine.

| G-code Instruction | Designated Operation |
|--------------------|---|
| E1P1/E1P0 | Laser On/Off |
| M3 S(0–1000) | Laser Ready + Set Laser Power (0–100%) |
| G1 X**** | Advance X axis by a millimetre value |
| G1 Y**** | Advance Y axis by a millimetre value |
| G1 Z**** | Advance build piston by a millimetre value |
| G1 A**** | Advance recoater by a millimetre value |
| M7/M9 | Rotate roller clockwise/anticlockwise |
| G1 B**** | Advance feed piston 1 by a millimetre value |
| G1 C**** | Advance feed piston 2 by a millimetre value |

7. Validation and characterization

The validation of the SLS machine was performed in two parts. The first part evaluated the individual components and operations of the machine such as the stepping accuracy, optical power supplied by the laser and laser spot size. The second part examined the geometrical accuracy, density and mechanical (tensile) properties of parts produced from polyamide-12.

7.1. Characterization of Machine components

7.1.1. Positioning accuracy

The accuracy of the positioning of the laser and build platform are key contributors to obtaining parts which exhibit high levels of geometrical resemblance to the model data. Therefore, it was important to characterize the variation in the positioning of the laser and the built platform. To characterize the registration error in the movement of the laser in the X and Y planes and the build platform in the negative Z direction, a dial indicator (Mitutoyo, Tokyo, Japan) with a measurement resolution of 0.01 mm was used (Fig. 35).

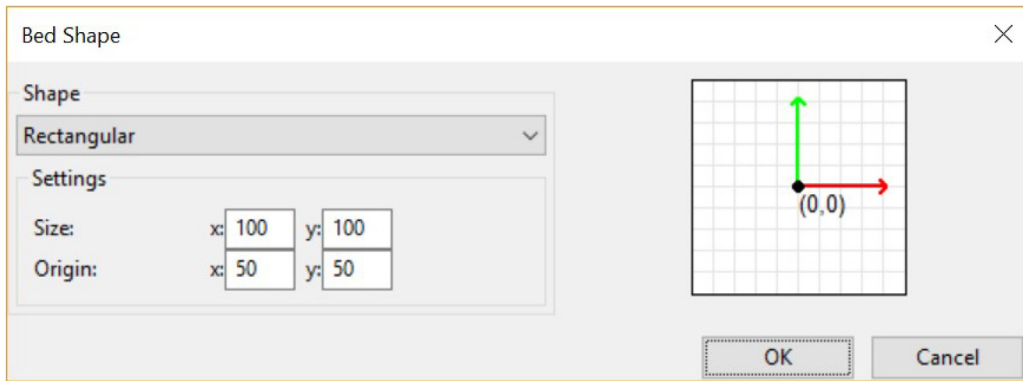


Fig. 31. Slic3r bed shape.

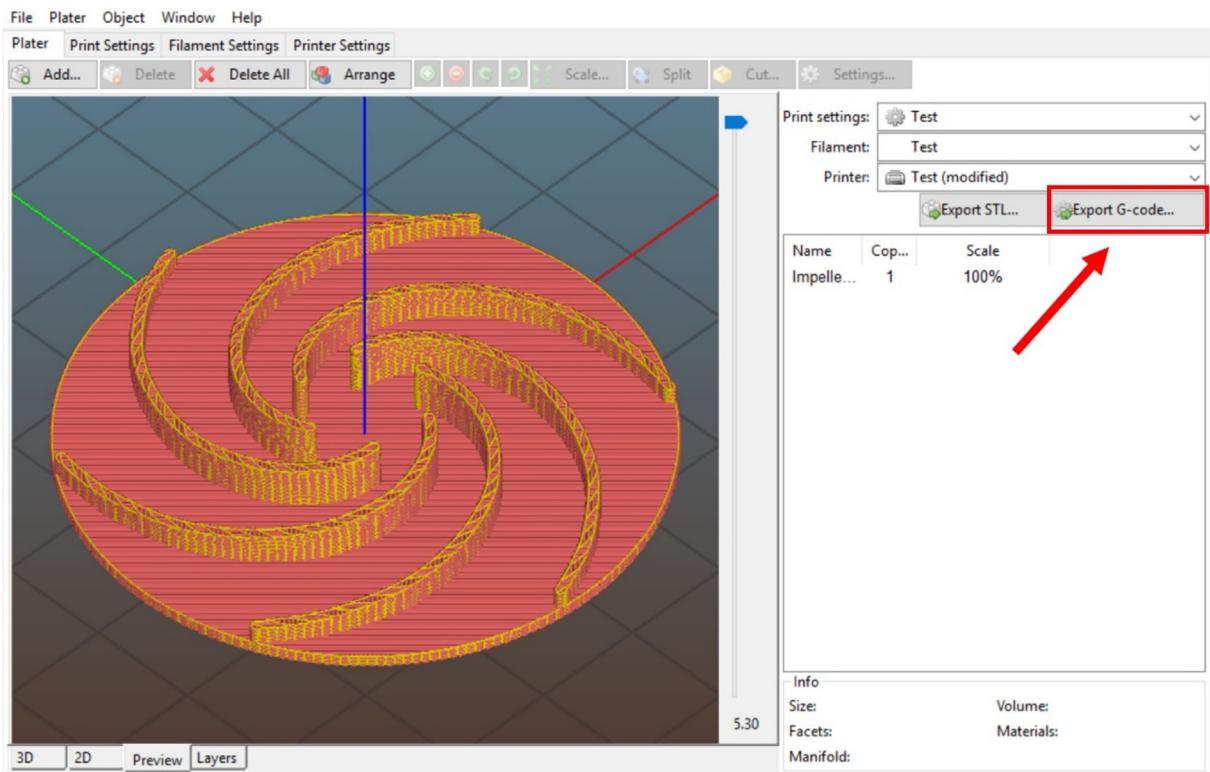


Fig. 32. Slic3r workspace preview with model inserted (a small pump impeller).

The dial indicator was placed parallel to the direction of movement for each axis. Using the machine's software interface, the X and Y axes were traversed between 2.5 and -2.5 mm in steps of 0.1 mm while the position on the dial gauge was recorded at each interval. As backlash was not an important characteristic of the build piston as it was always moved in the negative Z direction, it was traversed between 0 and -5.0 mm in steps of 0.1 mm. The acquired positional data for each axis can be found in Fig. 35, Fig. 36 and Fig. 37 for the X-axis, Y-axis and Z-axis respectively.

The positional data for both the X-axis and Y-axis (Fig. 35 & Fig. 36) show that there was some registration error in the drive mechanism which was a major contributor to the absolute average error of both axes which was calculated to be 0.016 mm and 0.021 mm respectively (Table 3). However, as mentioned previously, the maximum theoretical accuracy of a part produced using SLS is half the diameter of the largest particle in the powder used. With this being the case, it can be seen that with the absolute average error being less than half of the average particle diameter ($D_{50} = 43 \mu\text{m}$), the positional accuracy of the laser is not a limiting factor of part accuracy in the X-axis and Y-axis. Results in Fig. 37 demonstrate that the

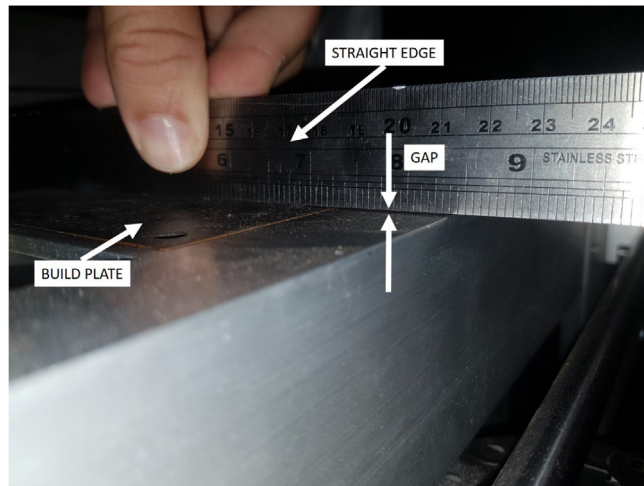


Fig. 33. Zeroing the build piston with a straight edge.

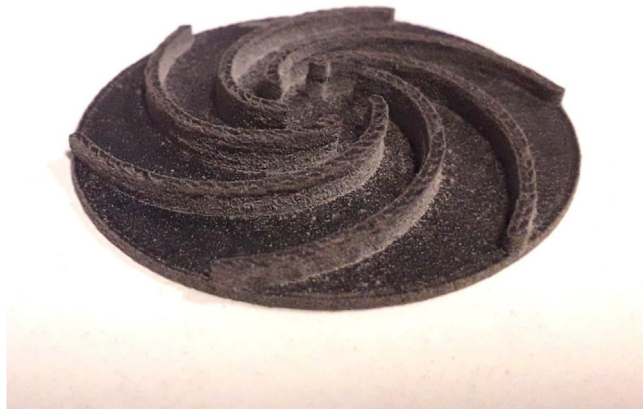


Fig. 34. Finished polyamide-12 impeller.

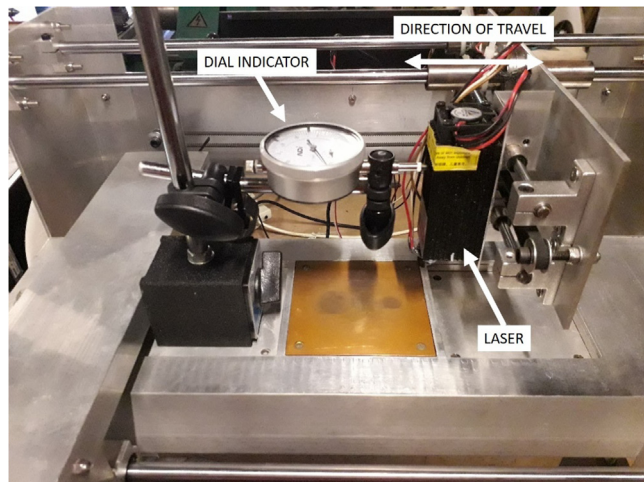


Fig. 35. Dial gauge set up to measure the positional accuracy of the X axis.

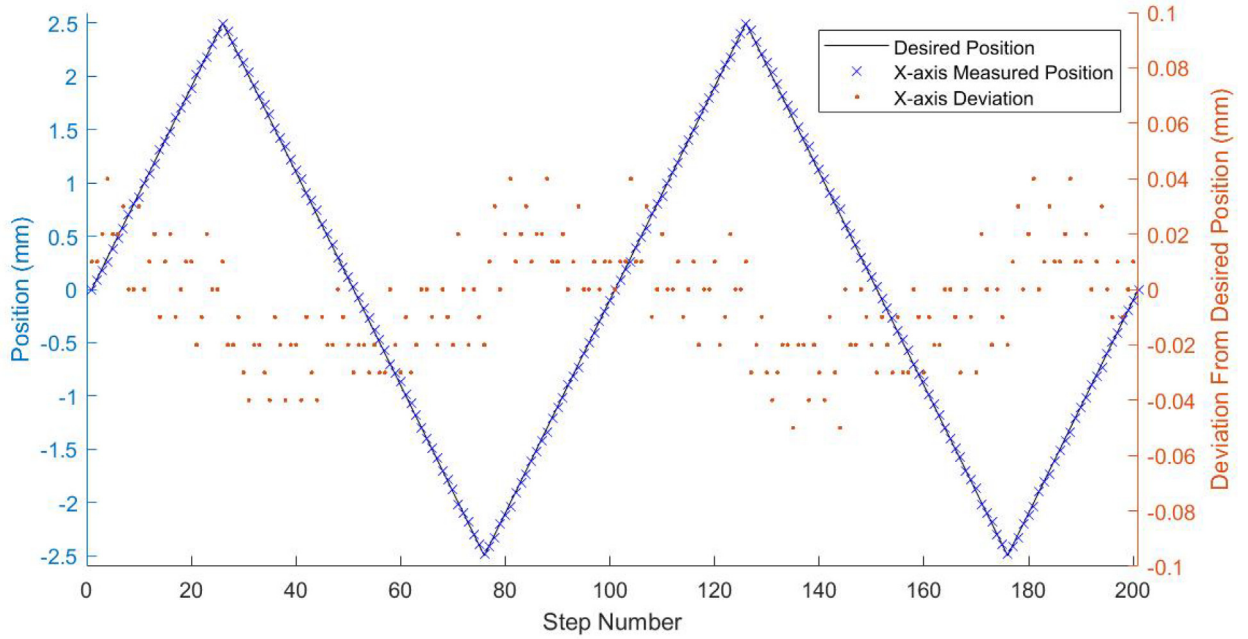


Fig. 36. Recorded positional data for X-axis.

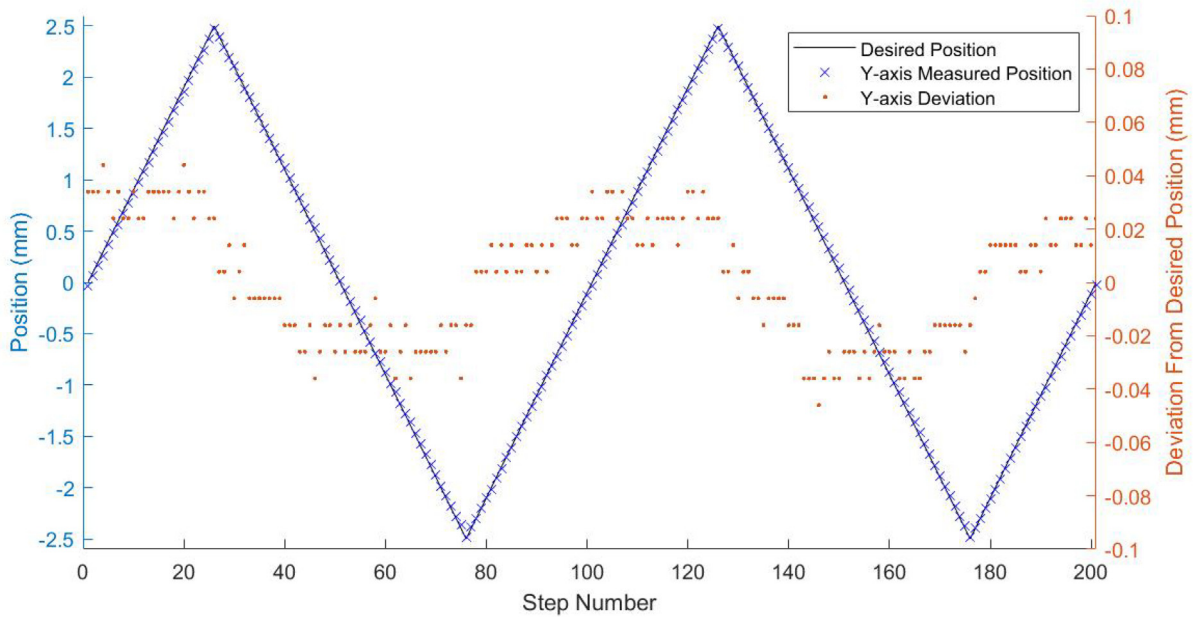


Fig. 37. Recorded positional data for Y-axis.

Table 3
Summary of positional error statistics for all axes.

| Axis | Absolute Average Error (mm) | Standard Deviation (mm) | Percentage Error <= 0.1 mm | Percentage Error <= 0.2 mm | Percentage Error > 0.2 mm |
|------|-----------------------------|-------------------------|----------------------------|----------------------------|---------------------------|
| X | 0.016 | 0.020 | 36% | 59% | 41% |
| Y | 0.021 | 0.025 | 20% | 47% | 53% |
| Z | 0.005 | 0.008 | 77% | 100% | 0% |

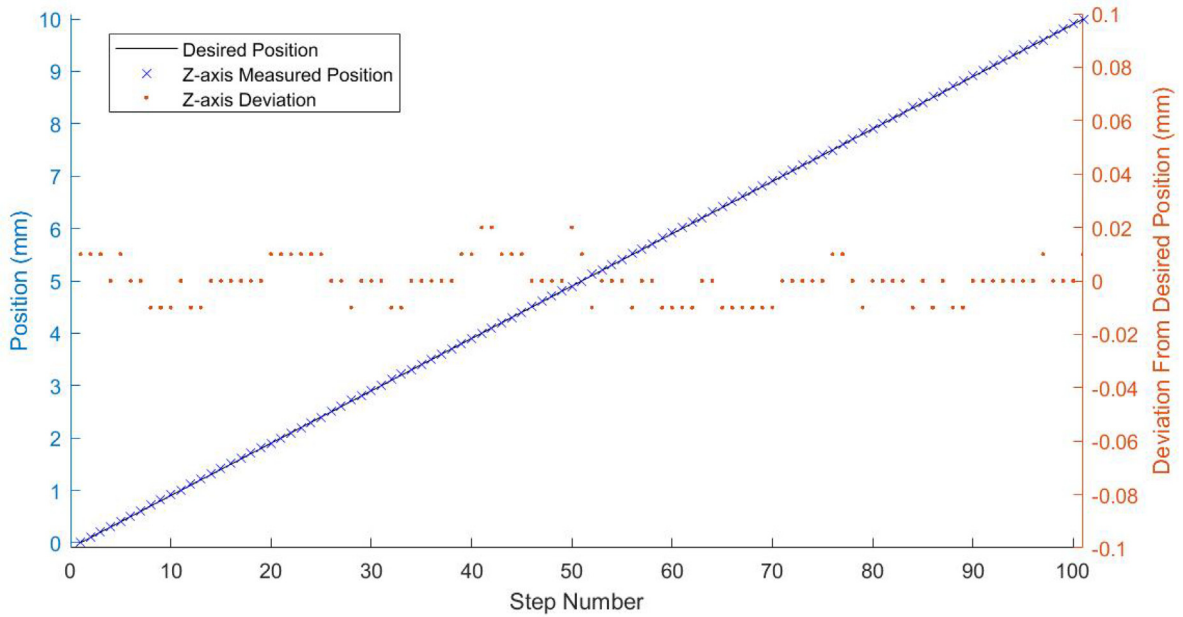


Fig. 38. Recorded positional data for Z-axis.

positioning accuracy of the build piston far exceeds that of the other axes with an average absolute error of 0.005 mm (Table 3). Again, this indicates that the positional accuracy of the Z-axis is not a limiting factor in part accuracy and will assist in controlling the uniformity of transmitted laser energy between layers.

7.1.2. Laser power measurements

To accurately determine the optical energy supplied by the laser, the output power was measured using a 15 W average laser power meter (UP19K-15S-W5-D0, Gentec Electro-Optics Inc., Quebec, Canada) calibrated to the wavelength of the laser.

The laser was mounted 50 mm from the power meter to minimise the amount of light scattered by particles in the air (Fig. 38). An Arduino (Mega 2560, Somerville, Massachusetts, USA) was used to supply a PWM signal with a variable duty cycle to the laser's constant current controller and the voltage and current supplied to the diode was monitored using two digital multimeters. The PWM signal was varied between 5% and 100% duty cycle in steps of 5% which operating in continuous wave mode. The optical power, voltage and current measurements were taken after 60 s of continuous operation at each data point to allow the diode to reach operating temperature. The results were then used to determine the required supplied PWM duty cycle for the desired optical power output.

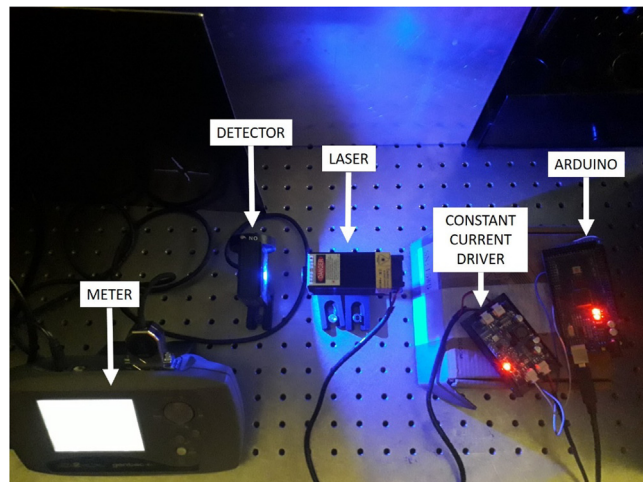


Fig. 39. Setup of the experiment to measure laser input and output power.

The results from the laser power measurements (Fig. 39) show that the optical power output of the laser linearly increases with the increasing duty cycle of the PWM signal until 80% where the output reaches a maximum of 2.44 W. Further increases in the duty cycle of the PWM signal appear to result in a linear decrease in optical power. The likely cause of this is overheating of the PN junction of the laser diode causing it to increase its resistance resulting in decreased optical power [5]. From this it can be determined that the duty cycle of the PWM signal should be kept to 80% or lower to avoid damage to the laser diode through overheating.

7.1.3. Laser spot size

To determine the minimum scan spacing value, the laser spot size was measured. Usually this measurement would be performed using a beam profiler, however due to the high cost of these machines, it is likely that not all researchers would have access to this measurement technique. Therefore, a simple procedure involving the marking of a material using the laser and then measuring the width of the mark was employed. To perform this measurement, the laser was made to mark a piece of medium-density fibreboard with a series of 20×20 mm boxes which was placed at the same focal distance as the powder layer from the laser. A calibrated digital microscope was then used to capture high resolution images of the markings which were then post processed using ImageJ (National Institutes of Health, Bethesda, Maryland, USA) determine the spot size (Fig. 40).

From measurements taken by scaling the pixels of the microscope using the supplied calibration grid (Fig. 40b), the laser spot size was calculated to be 0.35 mm in both the X and Y planes. This indicates that the minimum scan spacing required for 100% infill of parts is 0.35 mm.

7.2. Characterization of produced parts

7.2.1. Feedstock

The feedstock chosen for processing using this SLS machine was a polyamide-12 powder (SP301, Guangdong Silver Age Sci. & Tech. Co. Ltd., China) produced using precipitation. The powder was designed specifically for a machine equipped with a laser emitting radiation with a short wavelength (towards ultraviolet) which involved increasing the optical absorption in that spectrum by the addition of tinting dyes. The resulting powder had a near spherical particle morphology (Fig. 41).

A summary of the material characteristics, as reported in the datasheet provided by the manufacturer, can be found in Table 4.

The particle size distribution (Fig. 42) shows a near normal monomodal distribution about the D_{50} of the powder.

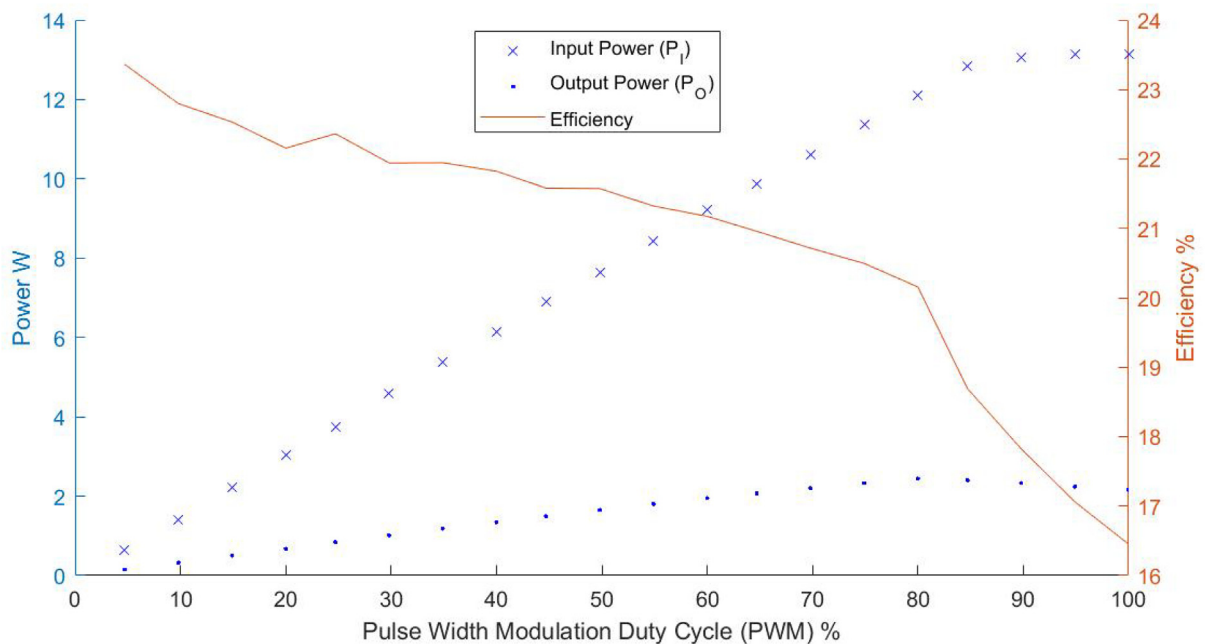


Fig. 40. Laser input and output power measurements with calculated efficiency.

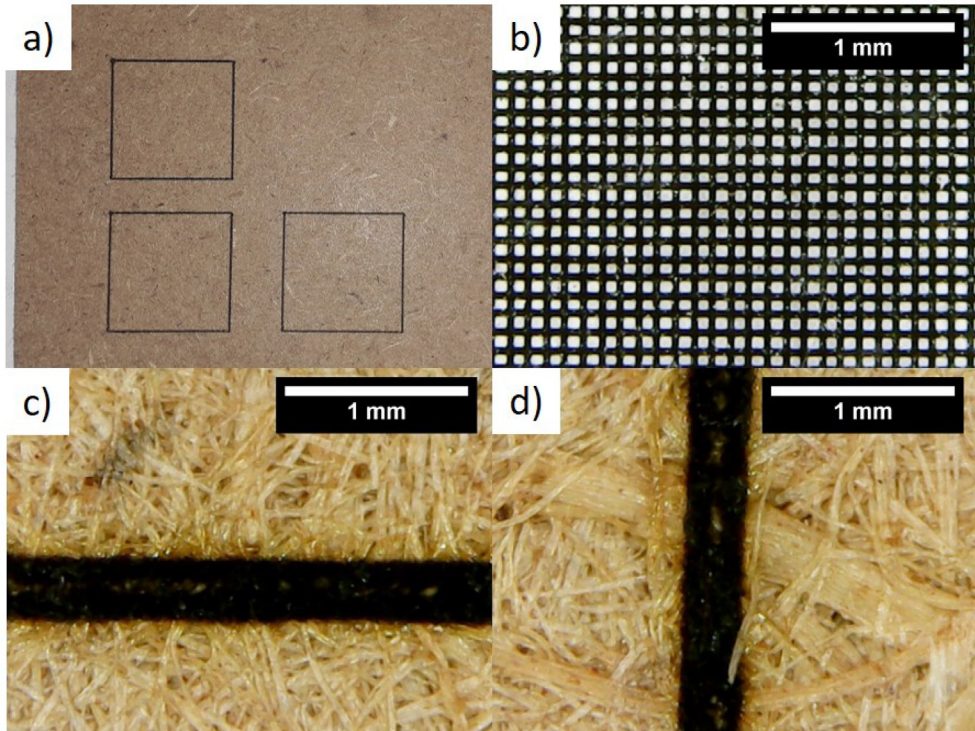


Fig. 41. a) Macroscopic image of the square burnt by the laser and microscopic images of the b) calibration grid, c) horizontal section and d) vertical sections of the square.

Table 4

Feedstock material characteristics.

| Powder | Theoretical Density (ρ_T) kg/m ³ | Bulk Density (ρ_B) kg/m ³ | Crystallisation Temperature (T_c) °C | Melting Temperature (T_m) °C | Median Particle Diameter (D_{50}) μ m |
|------------------|---|--|---|-------------------------------------|--|
| SP301 (Black) | 960 | 420 | 146 | 185 | 43 |

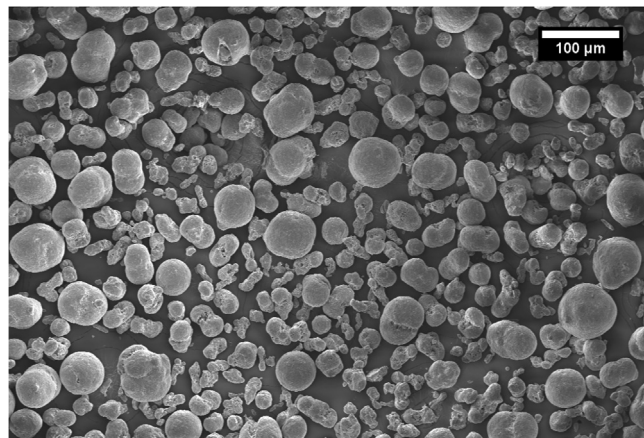


Fig. 42. An SEM image of the polyamide-12 powder.

7.2.2. Processing parameters

In literature, the primary processing parameters used in the SLS process are described by the layer height and the supplied energy density per unit area (Eq. (1)) [3].

$$E = \frac{P}{SS \times SP} \text{ J/mm}^2 \quad (1)$$

where P is the laser power in watts, SS is the scan speed and SP is the scan spacing in millimetres.

To simplify the experimental determination of the required input energy, some parameters were fixed to some commonly used values. The layer height was selected to be 0.1 mm which is a value often reported in literature [3] and the scan spacing was set to the diameter of the laser spot (0.35 mm) so that there was no spacing between adjacent infill scans. The scan speed was set to 29.17 mm/s (or 1800 mm/min in Mach3). Once those values had been set, there was only one variable that could be altered which was laser power. Laser power was varied between 20% and 50% of the total power available in steps of 5% to deliver supplied energy density values of between 0.06 J/mm³ and 0.16 J/mm³. The scan strategy was set to rectilinear fill and the build plate was set at 180 °C which is just below the melting temperature of the polyamide-12 material.

7.2.3. Measurements

For geometry and density measurements, four cuboids were produced at each energy level. Each produced part was measured in all planes using a digital caliper conforming to DIN 862 (Kincrome, Scoresby, Australia). The digital caliper was factory calibrated to ± 0.01 mm giving a maximum volumetric measurement error of 0.35%. The mass of each part was measured using a precision scale (GR-200, A&D Company Limited, Tokyo, Japan) allowing the density of each part to be calculated. Mechanical testing was performed as per ASTM D638 with type V (Fig. 43) tensile test samples (N = 4). An Instron (3367, Norwood, Massachusetts, USA) tensile test machine was used fitted with a 5kN load cell. The extension rate was set to 0.005 mm/s.

8. Results

Results show that an increase in energy density per unit area (Fig. 44) causes a somewhat predictable increase in part size in the X-Y plane. This can be explained by excess energy being conducted to adjacent particles in the powder bed [6].

Fig. 45 shows part density increasing almost linearly to a maximum density of 920 kg/m³ at a supplied energy density per unit area of 0.129 J/mm². This corresponds to a part density of 96% of the theoretical density of the material.

The reduction in part density due to a further increase in supplied energy density has been noted previously [6,7]. This can be explained by an excess in thermal energy causing particles which are adjacent to the laser spot being attached to the part without undergoing full melting. It is therefore determined that the optimum energy to be supplied by the laser to achieve the highest part density without the risk of excess grain growth is 0.129 J/mm².

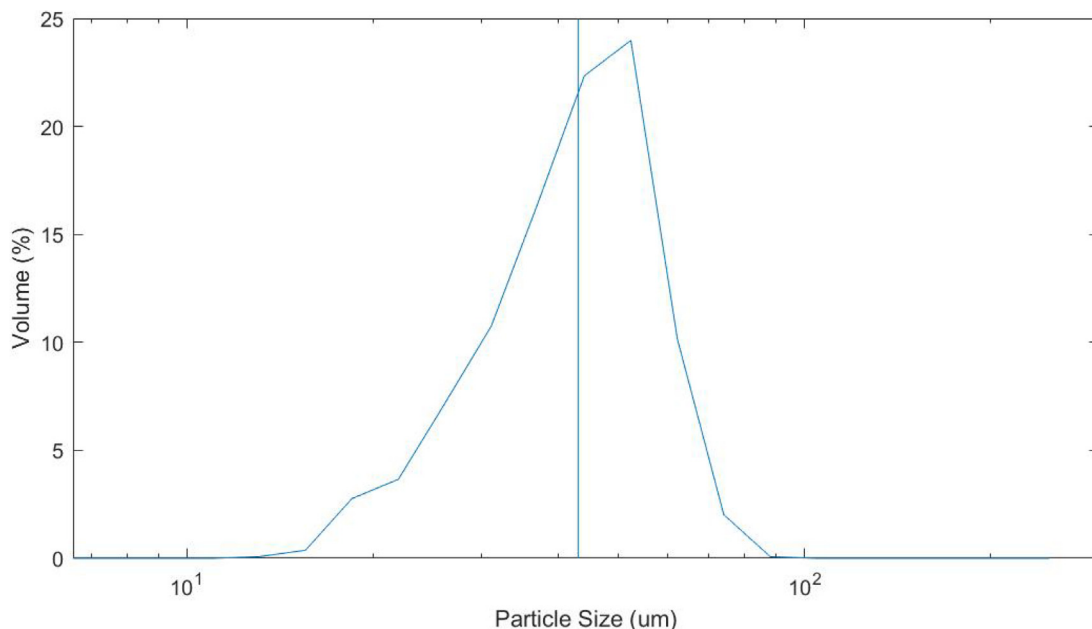


Fig. 43. Particle size distribution of the polyamide-12 powder.

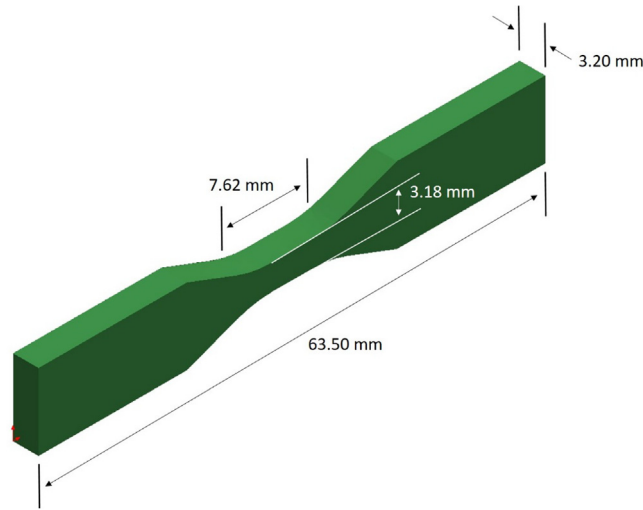


Fig. 44. Dimensions of the ASTM D638 Type V tensile specimens.

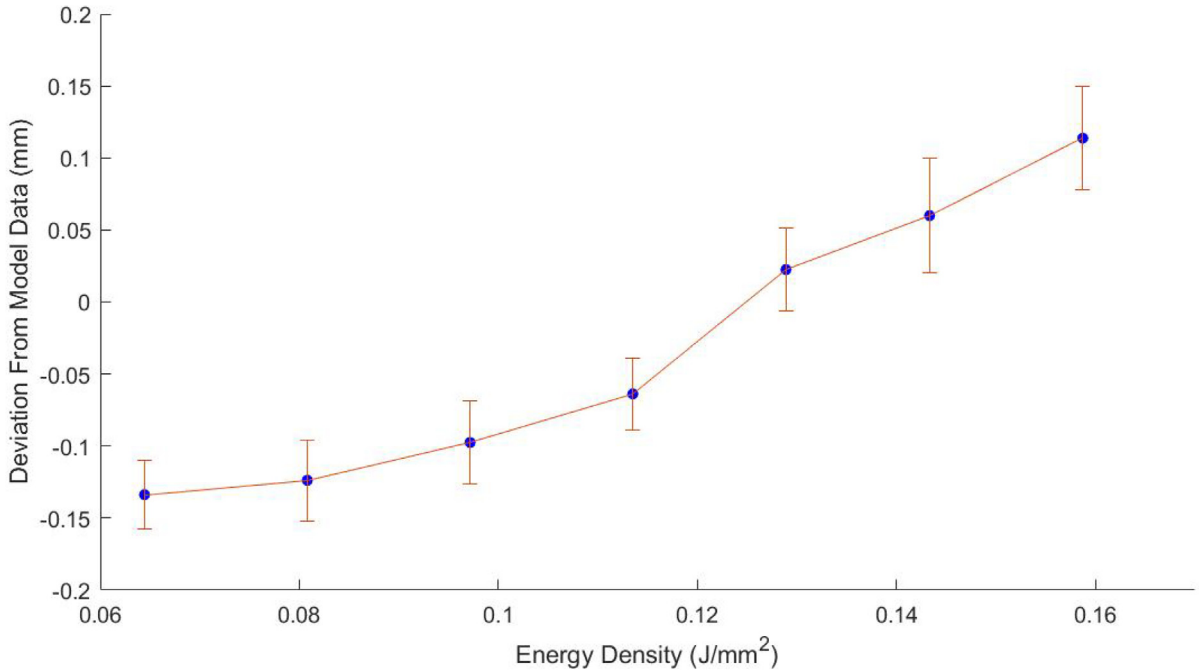


Fig. 45. Part deviation from model data in the X-Y plane as a function of supplied energy.

When the mechanical properties are examined against the supplied energy density (Table 5 and Figs. 46 & 47), elastic modulus indicates that the material becomes more brittle as the energy is increased. This indicates that an increase in the thermal gradient in the material makes it more resistant to deformation. However, when the elongation at the material's failure point is examined against supplied energy density, it shows that a maximum value of $11.13 \pm 0.02\%$ is reached at an energy density of 0.129 J/mm^2 . When the supplied energy exceeds this value, the failure point is reduced (Fig. 48).

Table 5
Mechanical properties of the produced samples.

| Supplied Energy (J/mm ²) | 0.064 | 0.081 | 0.097 | 0.114 | 0.129 | 0.143 | 0.156 |
|--------------------------------------|--------------------|-------------------|-------------------|-------------------|-------------------|--------------------|--------------------|
| Elongation at Break (%) | 6.77 ± 0.50 | 7.77 ± 0.22 | 9.24 ± 0.92 | 11.03 ± 0.10 | 11.13 ± 0.02 | 10.06 ± 0.14 | 9.24 ± 0.32 |
| Elastic Modulus (MPa) | 177.44 ± 12.08 | 280.73 ± 6.04 | 257.58 ± 4.48 | 307.11 ± 8.03 | 358.36 ± 3.04 | 373.20 ± 16.58 | 385.90 ± 14.63 |

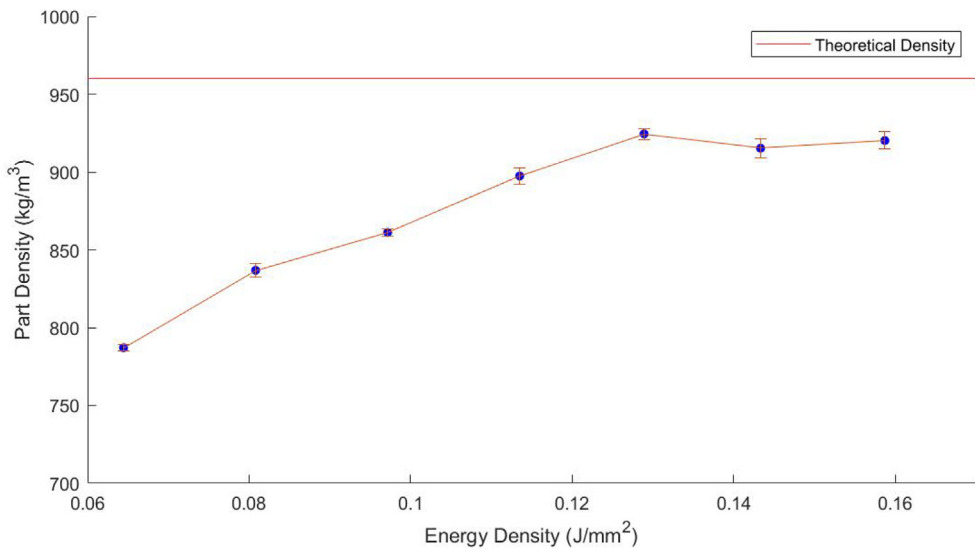


Fig. 46. Part density as a function of supplied energy.

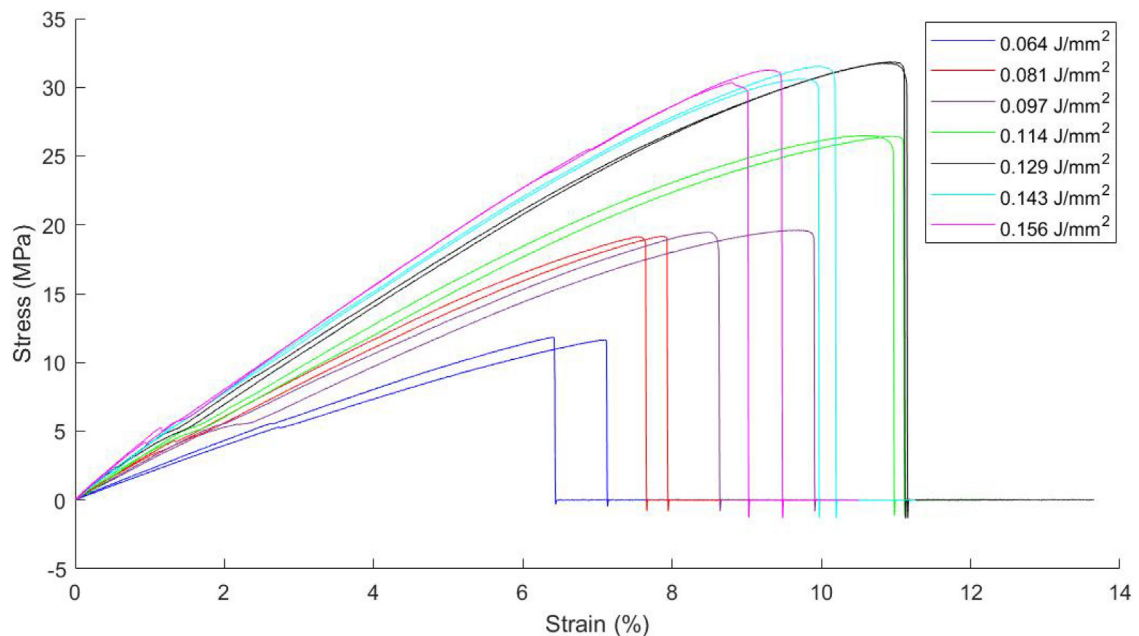


Fig. 47. Stress vs. strain curves for samples from each tested power level.

In this part characterization section, it was demonstrated experimentally that the supplied energy density could be varied and that this variation affected part growth in the X and Y planes, part density and mechanical properties. From the results of varying the supplied energy density, an upper limit (0.129 J/mm^2) was chosen which represented the highest part density ($918 \pm 9 \text{ kg/m}^3$) and mechanical properties (elastic modulus of $358.36 \pm 3.04 \text{ MPa}$ and elongation at break of $11.13 \pm 0.02\%$). Furthermore this machine has been used to produce permanent magnets by processing mechanically alloyed neodymium-iron-boron and polyamide-12 powders [8]. The successful processing of these alloyed materials demonstrates one of the potential uses for this machine within a research environment.

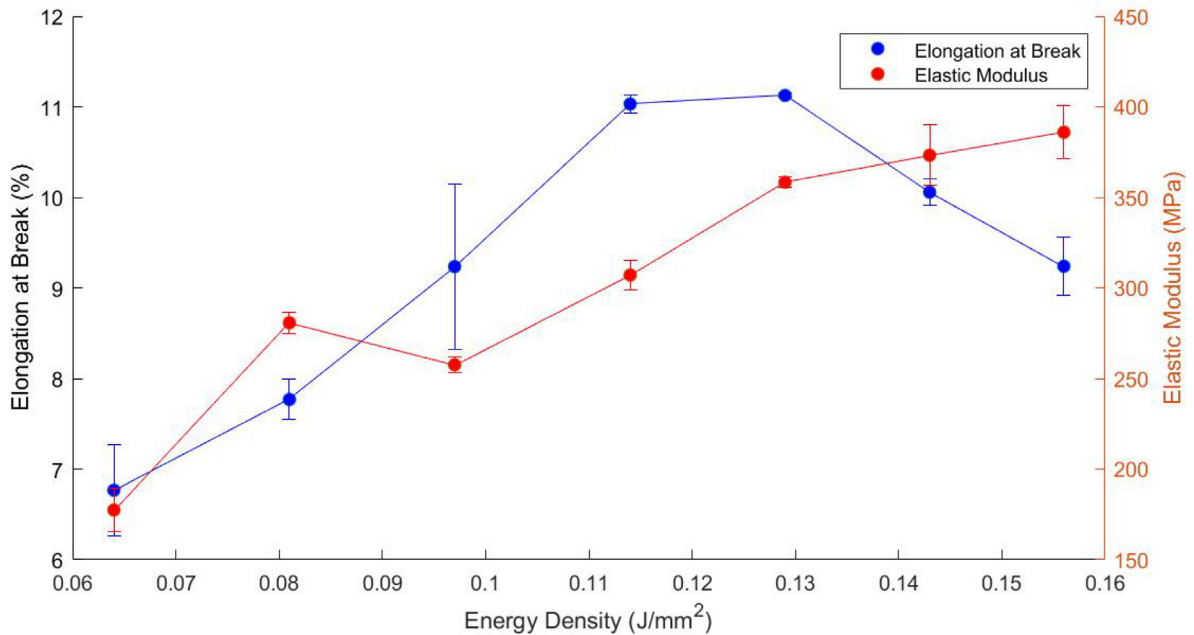


Fig. 48. Elongation at break and elastic modulus as a function of supplied energy.

9. Human and animal rights

No human or animal studies were conducted in this work.

Funding

This work was supported by the Prince Charles Hospital Foundation, Brisbane, Australia [NI2017-28].

Declaration of Competing Interest

The authors declare that they have no known competing financial interests or personal relationships that could have appeared to influence the work reported in this paper.

References

- [1] T.T. Wohlers, Wohlers Associates Inc., Wohlers report 2009: state of the Industry: Annual Worldwide Progress Report, Wohlers Associates, 2009, ISBN 0-9754429-5-3.
- [2] G.M. Vasquez et al, A targeted material selection process for polymers in laser sintering, *Addit. Manuf.* 1–4 (2014) 127–138.
- [3] I. Gibson, D. Rosen, B. Stucker, *Additive Manufacturing Technologies: 3D Printing, Rapid Prototyping, and Direct Digital Manufacturing*, 2nd ed., Springer New York, New York, NY, 2015.
- [4] Coslow, T. 2019 SLS Printer Guide - All You Need to Know. [Accessed on 19/08/2019] Available from: <https://all3dp.com/1/best-sls-3d-printer-desktop-industrial/>.
- [5] Y.Y. Kalisky, I. Ebrary, *The Physics And Engineering Of Solid State Lasers*, SPIE Press, Bellingham, Wash, 2006.
- [6] B. Caulfield, P.E. McHugh, S. Lohfeld, Dependence of mechanical properties of polyamide components on build parameters in the SLS process, *J. Mater. Process. Technol.* 182 (1) (2007) 477–488.
- [7] I. Gibson, D. Shi, Material properties and fabrication parameters in selective laser sintering process, *Rapid Prototyping Journal* 3 (4) (1997) 129–136.
- [8] M. Mapley et al, Selective laser sintering of bonded magnets from flake and spherical powders, *Scr. Mater.* 172 (2019) 154–158.